Volume 18 | Issue 5 | October 2021

MINING & QUARRY WORLD

Volume 18 • Number 5 • October 2021

CONTENTS

Features

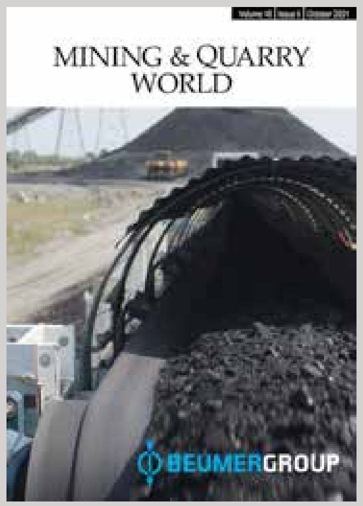

BEUMER Group offers a comprehensive product and system solutions portfolio to customers from the coal mining industry. Conveying technology includes closed Pipe Conveyors and open troughed belt conveyors that can be adjusted to the respective situation. As a system supplier, BEUMER Group also provides extensive know-how and the necessary components for storing hard coal, e.g. stackers and bridge reclaimers.

Managing Director and Publisher: Trevor Barratt

International Sales:

Gordon Barratt	+44 1909 474258	gordon.barratt@tradelinkpub.com
Gunter Schneider	+49 2131 511801	info@gsm-international.eu
Graphic Designer:	Sarah Beale	sarah@g-s-g.co.uk

Published by: Tradelink Publications Ltd.
16 Boscombe Road, Gateford Worksop, Nottinghamshire S81 7SB

Tel: +44 (0) 1777 871007
+44 (0) 1909 474258
E-mail: admin@mqworld.com
Web: www.mqworld.com

All subscriptions payable in advance.
Published 6 times per year, post free:
UK: £60.00 **Worldwide:** £70.00 | ISSN No: 2045-2578 | D-U-N-S No: 23-825-4721

New Komatsu D475A-8 mining dozer delivers more production and longer life

On mining sites, support machines, like dozers, can directly impact productivity by keeping blasting, loading and dump areas clean, enabling loading and hauling equipment to work more efficiently. If your operation needs a versatile mining dozer that can go from ripping solid rock to cleaning up around the dragline, take a look at the new Komatsu D475A-8.

Built for years of reliable service

Using extensive customer feedback, Komatsu re-engineered the D475A-8 mainframe to target twice the life of previous models and withstand multiple rebuild/overhaul cycles. Its low center of gravity provides machine stability and long and consistent track on ground length offers more traction, pushing power, ripping efficiency and less shoe slippage. Track shoe slip control automatically controls engine speed and minimises slip during ripping.

- Operating weight: 115,300 kg (254,193 lbs.)
- Net horsepower: Forward – 664 kW @ 2,000 rpm (890 HP @ 2,000 rpm)
- Net horsepower: Reverse – 722 kW @ 2,000 rpm (968 HP @ 2,000 rpm)
- Blade capacity: 27.2-45.0 m^3 (35.6-58.9 yd^3)

Additional horsepower can provide for faster ground speeds, shorter cycle times and more production tons per hour, when appropriate. The D475A-8's high horsepower in reverse means the lock-up converter stays engaged more frequently, allowing significantly higher levels of production, especially when pushing down slopes.

Increased production; less fuel consumption

Engineered for exceptional production, the D475A-8 mining dozer is designed for power, stability and solid performance. Komatsu's lockup torque converter produces a more efficient transfer of power to the driveline, designed to help decrease cycle times and increase production. During long pushes, the automatic gearshift mode allows the system to automatically engage the torque converter lockup clutch. Locking up the torque converter transmits all the engine power directly to the transmission, increasing ground speed and thus achieving efficiencies equal to a direct drive, consuming less fuel.

- Up to 10% productivity increase over previous models
- 11.5% more engine power in reverse, compared to forward direction
- 10% reduction in fuel consumption with automatic transmission with lockup torque converter compared to manual gearshift operation

Improved operating environment

Improvements to the

operator's cab make the D475A-8 more comfortable to operate throughout long shifts. Ergonomically placed touch points and palm control joysticks make operation easier. Outstanding operator visibility to the ripper shank, a rear view monitoring system and a heated, ventilated, air-suspended seat help keep operators comfortable. The redesigned undercarriage of the D475A-8 drastically reduces shock and vibrations when the dozer travels over rough terrain.

Doze with a blade built for efficiency

Operators can boost efficiency by working in blade auto-pitch mode, designed to increase dozing efficiency while reducing the amount of operator input required. The all-new blade support structure is designed to significantly reduce blade side sway. It also has fewer maintenance points and enhances operator visibility to the blade.

Maintenance features

The D475A-8 is engineered to minimise planned downtime and make maintenance efficient with features such as centralised greasing points, ground-level fill/evac service center and battery and starter isolators with lockout tagout functionality.

For additional information about the D475-8, please visit the Komatsu website.

About Komatsu

Komatsu is an industry-leading manufacturer and supplier of equipment, technologies and services for the construction, forklift, mining, industrial and forestry markets. For a century, Komatsu equipment and services have been used by companies worldwide to develop modern infrastructure, extract fundamental minerals, maintain forests and create technology and consumer products. The company's global service and distributor networks support customer operations, tapping into the power of data and technology to enhance safety and productivity while optimizing performance.

Heap leaching – an economical solution

Heap leaching is a low-cost technology used in industrial mining to recover precious metals such as gold and uranium, along with several other highly sought-after metals like copper, from their primary resources (ores and minerals). For many decades, there has been a growing demand for heap leaching due to its environmental benefits. Heap leaching provides mining operators with a benign, effective, and economical solution for the environment and produces only minor emissions from furnaces. The cost of the heap leaching process is low, making this process an attractive option from a financial standpoint.

Heap leaching is one of the oldest and the most traditional mining processes used to extract the valuable metals from specific minerals. Basically, this is a hydrometallurgical process in which the solution is applied for the dissolution of minerals from the ore that is used for the extraction of metals. Originally, heap leaching was practiced 500 years ago. Georgius Agricola published a book De Re Metallica in 1557 and reported that the heap leaching process was finished in a 40-day cycle.

Since the middle of the 16th century, heap leaching was practiced in Hungary for copper extraction. In 1969, gold heap leaching began in Nevada (birthplace of modern heap leaching) and in the middle of the 20th century, the United States Bureau of Mines began applying this technology. Gold and silver heap leaching first began at Cortez in 1969. Currently, 37 different heap leaching operations are active worldwide to produce gold, which is estimated to be around 198 tons per year.

Currently, new heap leaching operations are successfully commissioned throughout the world with the goal of treating mine tailings and residue and to establish effective waste management facilities.In recent years, 50 major heap-leaching, solvent-extraction, electro winning operations have been established throughout the world, and approximately three million tons of copper have been recovered, representing roughly 16% total copper production. The heap leaching technology developed thus far can be used for different types of ore. Advanced modelling studies and solid fundamentals of heap leaching technology could make the process more adaptable for increasingly composite ores.

Several factors are crucial for notable heap leaching operations, such as proper heap building and ore evaluations, efficient comminution methods, and feasible approaches to control the heap leaching process. There have been extensive reports and publications on current heap leach pad designs and construction practices. Current heap leaching methods were developed according to the industrial requirements. For example, heap leach ore depths were increased from 50-60 ft. to 500 ft. This function is significant for controlling the economic efficiency, surface area availability and for reducing the impact of mining reclamation on the environment. Heap leaching solution application rates are optimised for metal recovery with the minimal chemical consumption. The heap leaching process is very simple and thus offers greater economic feasibility over more expensive technologies. The motivation behind the use of heap leaching is financial feasibility.

The major advantage of the heap leaching method over conventional leaching and recovery techniques is that heap leaching consumes less than 0.3 ton of water for one ton of ore. Tank leaching normally operates as a continuous process within specially designed reactors. This approach is also known as a semi-closed system. Essentially, tank leaching is carried out in a set of tanks. In pressure leaching, finely ground ores are chemically treated at high pressures and temperatures within the reactors. The foremost application of the tank leaching method is the extraction of aluminium at low pressures and temperatures.The heap leaching process is obviously suitable method and has lot of advantages as mentioned above: however, as per the environmental concern it has some draw backs, such as time consumption, water loss,

accidental leakages of pregnant leach solutions, slow heap leach kinetics, and acid mine drainage problems (sulphide's).The objectives of this article are to provide information on the applications of a unique and versatile heap leaching process for rare earth extraction and to highlight the advantages and limitations of this process.

HEAP LEACHING OF MINES

Industrial mining processes are the activities involved in the extraction of metals or minerals. A good example can be the classical production process of iron sulphate. In this process, iron pyrite was heaped up and the leachate coming from the heap was collected and boiled with iron resulting in the production of iron sulphate. The basic processes involved in heap leaching are ore crushing, spreading the crushed ore over HDPE or PVC geomembrane-lined pads, and spraying a leaching solvent like sulfuric acid or cyanide over the pads so that valuable minerals will dissolve into the pregnant solution. Metal recovery is then performed through precipitation, smelting or electro-winning and absorption methods.

Generally, low-grade ores of valuable metals like gold, silver, and platinum are mined from the surface of the earth or sometimes subsurface of the earth, pulverised into tiny particles, and collected on to a dense leach pad. The heap leaching process involves several steps. First, a leach solution is used to irrigate the heap. The second step is interaction with the ore particles. Third, the precious metal leaches out of the solution. Fourth, the pregnant solution is collected, and finally, draining of the tailing areas is done for metal extraction. Lime, Portland cement, coal fly ash, and bottom ash, or other materials are mixed with crushed ore for agglomeration. In a few cases, after pulverization, sulphide ores can be treated via chlorination, bio-oxidation, roasting and autoclaving methods prior to the heap leaching process. In gold leaching, two similar types of leaching pads are used to maintain permanent heap operations. A summary of leaching methods used for the extraction of various metals is shown in **Table 1**.

Precious metal recovery by heap leaching, base metals from oxide ores, Zn, and gold recovery by heap bio oxidation. The main concern of this thesis was to understand the gold mineralizing process and the optimization of operational parameters during the bio-oxidation process. Basically, the low-grade ore was oxidised via the biological heap method, and later it was utilised as a supplementary feed. The heap leaching with computation process is a newly developed heap leaching methodology that combines analytical modelling and the Bernoulli type model to achieve a heap leaching scale up process. This method is very useful to optimise the heap leaching process (design, analysis, control and optimization) and also proposes optimal flow rates for the heap leaching process of gold, platinum group metals and base metals sequential heap leaching for platinum group metals, heap leaching with mathematical modelling for the extraction of copper was developed. In this paper, the authors reported the heap leaching plan and design for copper leaching by the mathematical model named MINLP and BARON-GAMS solver. They studied different primary variables such as acid price, variable costs, and ore grade quality. These were highly effective on the production capacity of copper.

Table 1: Summary of leaching methods for the extraction of different metals with recovery efficiencies.

Method	Extraction metal	Summary	Reference
Heap leaching	Precious metals from mineral fines	Leaching has been used principally in connection with low-grade copper ores or pit wastes.	Michael Kerr *et al*., 1998
Heap leaching	Base metals from oxide ores	75-82% of Nickel recovery was achieved in 160 days to 266 days, 90% Cobalt recovery was achieved in 14 days, Iron recovery (53.6%) was achieved in 198 days at ambient temperatures	Anthony *et al*., 2004
Heap leaching	Zn (Zinc)	The 95% of zinc recovery was possible in 16 days cycle at 25°C by column (heap) leaching.	Wen-qing *et al*., 2007
Heap leaching bio oxidation	Gold	49-61% of gold was recovery by bio oxidation process at 81°C. The bio oxidation process was for gold recovery was taken 150 days.	Wes K. Sherlock 2010
Heap leaching with computation process	Copper	71-73.5% of copper was recovery by developed a new heap leaching methodology with the combining analytical modelling at optimal flow rates.	Mario E. Mellado *et al*., 2011
Heap Leaching	Gold	30-95% of gold was recovery by best available technology heap leaching compared to other techniques.	Caner Zanbak., 2012
Heap leaching	Platinum group metals (PGMs) and base metals (BMs) from a low grade flotation concentrate of PGM concentrator plants.	The extractions of 52% Cu, 95% Ni and 85% Co were achieved in 30 days (65°C) by heap bioleach. If cyanide leach process (23°C) can be operated in 21 days, 20.3% Pt, 87% Pd and 46% Rh, if 50 days or more to achieve 50% platinum.	Mwase *et al*., 2012
Sequential heap leaching	Platinum group metals and particularly for palladium	At 65 °C, 93% Copper, 75% Ni and 53% Co extracted by bio heap leaching in the 304 days. By cyanide leach experiment, 57.8% Pt, 99.7% Pd and 90.3% Au was extracted at 50°C in 60 days.	Mwase *et al*., 2014
Heap leaching with mathematical modeling	copper	By the Mellado et al., method for the optimal design of heap leaching, 53-56% copper recovery was possible in a61-67 days.	Jorcy Y. Trujillo *et al*., 2014
Heap bioleaching	Cu, metal extracted from reduced inorganic sulfur compounds.	Over 60% of Cu, extraction was possible by bio heap leaching at 45 °C during the 30-48 days.	Watling *et al*., 2015
Heap leaching	Copper from ore	73% of Cu recovery was achieved in 140 days at 25 °C.	Rautenbach, 2015
Heap leaching for rare earths extraction	Heavy rare earths and Yttrium	91.3% and 87.2% of Yttrium and dysprosium achieved by heap leaching for 60 days, respectively, at room temperatures.	Pingitore Nicholas *et al*., 2016
Heap leaching with increasing flux rate	Gold	73-87% of gold extraction was achieved by using heap leach process with increasing flux rate in the 40 to60 days.	Ngantung, 2017
Heap leaching with the new model (MINLP) and GAMS software	Copper	69.7-76.7% of copper recovery was obtained from 19.5-43.5 days with the new mathematical modeling named mixed integer nonlinear programming (MINLP) including GAMS software (general algebraic modeling system).	Isis F. Hernández *et al*., 2017
Heap bioleaching	Nickel	60% recovery of nickel from the tailings for 110 days.	Anton Svetlov *et al*., 2017
Heap leaching with computational fluid dynamics model	Copper	55% of copper was recovered in the 700 days cycle at the temperatures from 12-45°C.	Diane McBride *et al*., 2018

Table 2: Comparison of capital expenditures (CAPEX) and operating expenses (OPEX) of copper, gold, and silver by heap leaching, tank leaching and autoclave methods.

Metal name	Heap leaching capital expenditure (CAPEX)US$/t ore	Heap leaching operating expenditure (OPEX) US$/t ore	Tank leaching capital expenditure (CAPEX)US$/t ore	Tank leaching operating expenditure (OPEX) US$/t ore	Autoclave leaching capital expenditure (CAPEX)US$/t ore	Autoclave leaching operating expenditure (OPEX)US$/t ore
Copper	29.5	4.6	25	66	75	19
Gold	22	4.51	40.9	22.28	492	8.20
Silver	22.50	14.87	40.9	35.96	17.40	82

It is possible to recover 60% of copper through heap bioleaching. The authors discussed an appropriate pad design for high leaching efficiency in the brief reviews on the heap pad designing criteria, pad characterization program, pad types, operational kinetics, material handling, and risk assessments. Finally, the authors concluded and recommended some technical tips for successful heap leaching facilities. Cu recovery of 73% was achieved in 140 days at 25°C. In 60 days, 91.3% and 87.2% of Yttrium and dysprosium were achieved by heap leaching, respectively, at room temperatures. The leaching processes with increasing flux rate for the gold recovery were also reported. Some brief reviews reported on the heap leaching of copper and gold. The main objective of this exclusive review paper is to understand the fundamental mechanism of the heap leaching process, as well the theoretical background of different heap leaching processes, global trend of commercial heap leaching operations, challenges, and the innovations and future directions of these process developments. This process is obviously suitable for low grade ores even if it has some draw backs. But it requires some comprehensive engineering concept developments for the higher efficiency of the product by heap leaching. Another brief review paper addressed a key technology for the recovery of valuable metals from low grade ores. The author covered heap leaching benefits, technical draw backs, economic feasibility, leaching kinetics, and environmental concerns.

Heap leaching with the new model (MINLP) and GAMS software, as well as the new model named mixed integer nonlinear programming (MINLP) including GAMS software (general algebraic modelling system) were utilised for the study of heap design and operational variables for metal recovery. It is one kind of a mathematical modelling applied for the copper leaching system. Recently, a heap bioleaching process was developed in Russia for the recovery of valuable copper and nickel from low-grade ore with a less expensive cost. In Russia, the Murmansk region required urgent research action for the mining wastes. In this region they developed the technology for the recovery of valuable copper and nickel from low-grade ore. During these mining activities, lots of wastes were deposited, so bio heap leaching technology was developed for the recovery of metals from ores with less expensive cost. Heap leaching with the computational fluid dynamics (CFD) model can analyse the heap design, operational parameters, optimization analysis and environmental conditions etc.

In the heap leaching process, initially the ore is pulverised and accumulated before it is placed on the heap to increase the mobility of the heap, as well as to maintain a high pH. Agglomeration involves the merging of the pulverised ore with binding material like ash, lime, Portland cement, or other materials. In few cases, pre-treatment of sulphide ores by bio-oxidation, autoclaving, roasting, or chlorination before heap leaching. There are two kinds of pad that are used in gold heap leaching, depending on whether the spent ore is removed or not: permanent heap construction on a pad and on-off pads. The former is the one which the leached ore is not removed from the pad and the latter has been where the spent ore is removed, and another fresh ore is allowed to be placed on.

HEAP LEACHING ADVANTAGES AND ECONOMIC FACTORS

Heap leaching has several advantages and economic benefits. These include low capital requirements and low operating costs; the absence of a milling step for crushing and agglomeration; the simplicity of atmospheric leaching; possible use for the treatment of moderate (medium) grade ores, (pebble size is ~31 mm with round shape), wastes and few deposits; and omission of liquid-solid separation step for counter-current operations, when metal tensor can do accumulate due to the use of the recycling solution over the heaps. Some ores which require crushing, agglomeration, and conveyor stacking may require little additional cost. The capital expenditures (CAPEX) and operating expenses (OPEX) of copper, gold, and silver by heap leaching, tank leaching of copper, gold, and silver and autoclave leaching of copper, gold, and silver are expressed in million dollars per ton of ore in **Table 2**.

HEAP LEACHING OF GOLD AND SILVER

Heap leaching is a very significant and common process in the copper and gold industry. It is very economical and useful for treating a wide range of low-grade ore bodies on a large scale. The simple heap leaching process is very competitive with other expensive laterite technologies. The Bureau of Mines reported the development of a gold ore heap leaching process which used a diluted cyanide solution for the gold and silver recovery from pregnant effluents by a carbon adsorption-desorption process. Hazardous waste engineering research laboratories submitted a report to the Environmental Protection Agency in the USA describing the great distribution and operational capabilities of the gold/silver heap leaching process and the potential environmental impact and management practices to minimise potential environmental releases. The basic processes involved in heap leaching are crushing the ore, spreading the crushed ore over HDPE or PVC geomembrane-lined pads, spraying leaching solvent like sulphuric acid or cyanide over the pads and then valuable minerals will dissolve into the pregnant solution. Metal recovery is then performed through precipitation, smelting or electro-

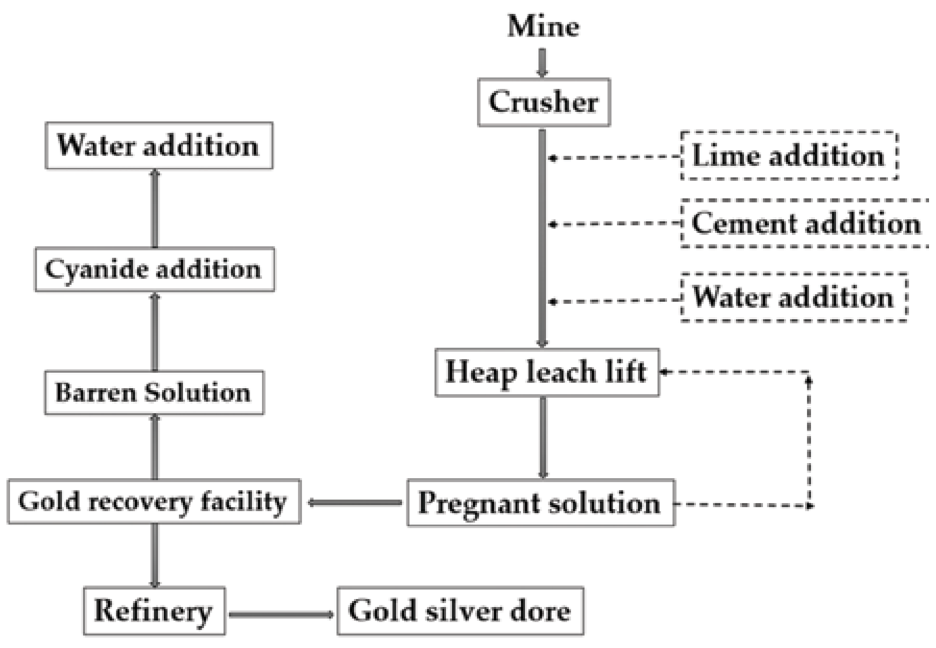

Figure 1: Chart of a gold heap-leach operation (adopted and modified from the reference 43).

winning and absorption methods. **Figure 1** shows a flow chart of a gold heap leach operation. A hydrometallurgical process has been designed for the amenable gold heap leaching from low-grade gold ore.

HEAP LEACHING OF COPPER

There are numerous reports available on copper heap leaching from copper ore. Some researchers have used heap leaching technology for the recovery of copper by using sodium nitrate as an oxidizing agent. The pH of the heap was maintained at pH < 1.7. Other investigations reported the heap leaching process of copper from diesel deposits. The non-ionic surfactant EVD61549 (a wetting agent) was used to increase the copper heap leaching efficiency. Heap leaching of waste copper ores from Volkovskoe deposits has also been considered for sulphuric acid leaching (25-75 kg/t ore). Over a period of three months, the copper leaching efficiency reached 76-78% overall. The copper recovery efficiency increased with an increase in the leaching time.

HEAP LEACHING OF URANIUM

Large-scale uranium heap leaching activities have operated since the 1970s and 1980s. Historically, sources of uranium ore contain ≥0.05% of uranium/thorium. In the 1950s and 1960s, ores containing less than 0.05% uranium were periodically refined in small heaps. There are three methods used for uranium recovery, namely: traditional milling, in situ recovery (ISR), and heap leaching methods. In the USA, heap leaching technology is widely used for the recovery of uranium. A rancher exploration and development corporation in Colorado was operated between 1977 and 1979. Some investigations reported bacterial leaching processes. Generally, problems arose during the oxidation of U+4 species, and approximately 70% could be recovered. Heap leaching technologies eliminate grinding, tank leaching and the solid/liquid separation step, and it is likely applicable to many types of low-grade uranium ore of many types. The conventional leach times are between one and six months. Recently, researchers reported the analytical models for the heap leaching by global sensitivity analysis and uncertainty analysis. **Figure 2** shows a flow diagram of gold, copper and uranium heap leach operation flow sheets.

RARE EARTH ELEMENTS RECOVERY BY HEAP LEACHING

Recently, rare earth appliances are significantly increased for new products. During the past 20 years, REEs have many new applications such as clean energy, petroleum refining, electronics, and automobiles. Military applications have also arisen as these materials are widely used in communication systems, avionics, lasers, precision-guided munitions, radar systems, satellites and night vision equipment (**Figure 3**).

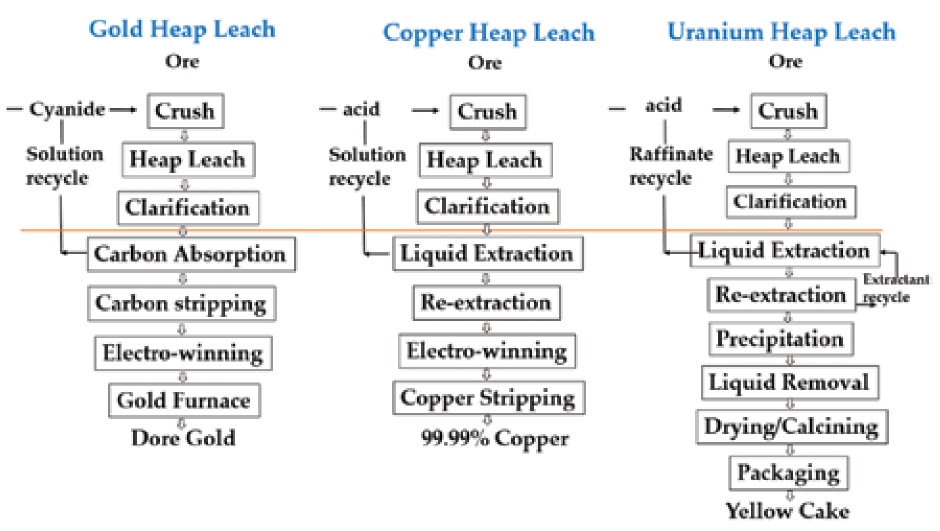

Figure 2: Flow diagrams of heap leaching processes of gold, copper, and uranium (adopted and modified from reference 54).

The assessment and source of REEs are in much interest, and advanced technologies are therefore required for the recovery of critical rare earths from waste residue via the heap leaching process. In the second generation of leaching technology, heap leaching with (NH4)2SO4 in the early 1980s was used to enhance the product purity to more than 92% for the total rare earth oxide content. During the washing process, the solid-to-liquid ratio was maintained at approximately 0.6:1 build upon the leaching time and heap size. Leaching times ranging from 100 to 320 h are more beneficial for rare earth extraction, with rates up to 90% realised.

Figure 3: Heap leaching for rare earth recovery.

Ion-adsorption clays from various origins or ores are rich sources of rare earths and the recovery process by in-situ leaching and heap leaching. 80% of the rare earths such as Y, Nd, Eu, Tb, and Dy were recovered by several process including physical separation, bio-oxidation, heap leaching, precipitation, and solvent extraction respectively. In 250 days, 85% of there're earths were leached with pH 0. When pH was increased to 3, rare earth recovery was observed to increase by two-fold. Texas rare earth resources independently confirmed a 79.9% recovery rate by the heap leaching process. Recently, heap leaching was applied for the recovery of the yttrium, from the ore yttrofluorite. Yttrium-bearing fluorite at Round Top Mountain is a rich source of Yttrium, and other heavy rare earth elements were recovered by the heap leaching process. In 60 days, 91.3% and 87.2% of Yttrium and dysprosium were achieved by heap leaching, respectively, at room temperatures.

Recently, the National Energy Technology Laboratory (NETL) funded the University of Utah and Virginia Technology for the extraction of rare earths from coal refuse by heap leaching, along with other sequential processes such as coal processing, bio oxidation, solution treatment, solvent extraction, and precipitation technologies respectively.

CONCLUSIONS

Heap leaching technologies have been profitably adopted for the recovery of highly sought-after metals. Worldwide, a huge interest in heap leaching projects has-been observed for the recovery of precious metals. Heap leaching is an essential metallurgical process which has demonstrated a strong potential to reduce costs and liberate metals from challenging deposits. Nowadays, prices for all precious metals and rare earths are increasing rapidly due to the continuous demand in green technology applications. Heap leaching is a more economic process than any other conventional method, and exceptionally so for the recovery of precious metals from low grade ore.

AUTHOR CONTRIBUTIONS

T.T., R.C., L.H., and L.Q.T collected the information, summarised, and wrote the manuscript. C.H.K. corrected the final manuscript and agreed to submit this data to the sustainability journal.

Australia and India take next step in mining partnership

Australia and India have discussed opportunities in coal technology, skills development, and business-to-business collaboration at a Joint Working Group (JWG) meeting on ‘Coal and Mines’.

The forum was co-chaired by Australia’s head of resources division Paul Trotman and India additional secretary, Ministry of Coal, Vinod Kumar Tiwari.

The delegates also discussed issues relating to India’s coking coal import from Australia.

Australia made presentations on its Global Resources Strategy as well as ways of leveraging technologies and infrastructure to decarbonise energy and industry.

Tiwari provided an overview of the coal sector in India, outlining the country’s current and future coal resources, while forecasting India’s critical and strategic minerals demand and supply scenarios.

Tiwari also explained the coal and broader mining priority areas the two countries could capitalise on going forward.

Other specific conversations included India and Australia’s collaboration on clean coal technology, surface coal gasification, coal bed methane, sharing of technology deployed for fire quenching, coal-based hydrogen, and carbon capture, utilisation and storage (CCUS).

An open house discussion was also held.

The JWG meeting was a precursor to the upcoming India-Australia Energy Dialogue – an annual meeting that will next take place on October 13.

The Energy Dialogue discusses the countries’ bilateral engagement on energy and resources.

Coal and Mines is one of four working groups established to support the forum, which also includes Oil and Gas, Renewable Energy and Smart Grids, and Power and Energy Efficiency units.

In June 2020, Australia and India announced a Memorandum of Understanding (MoU) on critical minerals.

The MoU has seen Australia take a significant step towards establishing itself as a reliable supplier of critical minerals for India’s growing manufacturing sector and its defence and space capabilities.

Innovative planning method for curved overland conveyors

Since the late 1960s, BEUMER Group has been developing and producing curved overland conveyors, making the company one of the pioneers in this industry. Nothing has fundamentally changed in the functional principles of this technology since then - except for the feasible limits: With highly developed core components, precise calculation methods and own planning tools, the system provider continues to push the limits of what is technically feasible - while drastically reducing the time and costs involved both in the planning phase and in the handling of projects.

"Our belt conveyors are able to solve complex problems with regard to the transport of any bulk material whether in the mining or cement industry," says Christoph Dorra, regional sales manager South America, Conveying and Loading Systems, at BEUMER Group. "While the basic task to transport bulk material from the material feed up to the final discharge point seems to be comparable, on closer inspection no system is similar to the other. The spectrum of potential conveyed materials alone requires individual consideration of the components to be used with regard to wear resistance or the maximum permissible gradients of a conveyor." In addition, the mass flow to be conveyed and the height to be overcome are the main factors determining the dimensioning of the drive unit of an overland conveyor. "A further challenge is posed by systems at high altitudes," says Dorra. At altitudes exceeding 4,000 metres, as it is often the case in the South American Andes, for example, it must be considered that the air pressure and thus the density of the air decreases with increasing altitude. This reduces both the cooling effect and the insulating capacity of the air. As a consequence, the drive units like frequency converters and electric motors do not achieve the specified rated power that applies for installation heights up to max. 1,000 metres above mean sea level. This is the so-called derating factor.

In addition to the pure material specification and the mass to be conveyed over a certain height, the topography along the conveying route is of particular importance in the project planning.

THE BIGGEST CHALLENGE: THE TOPOGRAPHY

"In 2009, we implemented an overland conveyor in China that is able to curve on 85 percent of the 12.5 km long conveyor line between the quarry and the cement plant. The system literally winds its way to the destination, without any transfer point," reports Dorra.

Potential obstacles appeared in the form of residential areas, roads and rivers that had to be crossed, larger bodies of water or mountains that could not be crossed. "Not everyone would automatically think of an overland conveyor as the optimal solution when faced with these challenges," says Dorra. "But for us, these projects are a special attraction. Our target is to have as few transfer points as possible along the entire conveyor line". This reduces both wear and tear and the environmental impact of dust, for example, but also increases the availability of the overall system and significantly improves ease of maintenance.

FOUR STRAIGHT CONVEYORS ARE CONVERTED TO ONE BEUMER OVERLAND CONVEYOR

A good example for such challenges is represented by the project of an American coal mine. Here, a BEUMER overland conveyor with a length of approx. 6.5 kilometres conveys coal from a new underground mine portal to its main coal prepration plant. In the original request for quotation, the client requested four straight conveyors where three transfer towers would have been needed. For BEUMER Group, there was clear potential

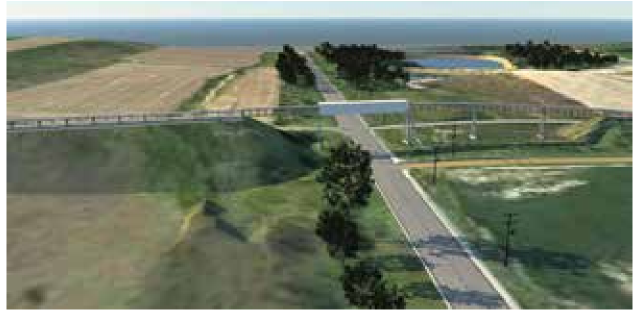

for optimisation here, of which the system provider was able to convince the customer.

The BEUMER team was also faced with exciting challenges in a Belgian project. Since the 1970s, the residues of a coal-fired power plant were landfilled on a fly ash stockpile. It was intended to transform the terrain into a nature park. In order to make this possible, the fly ash had to be conveyed to the Mass river, about two kilometres away, where it is loaded onto ships for further transport. These bring the fly ash downstream to an adjacent cement plant, where it is recycled as an aggregate.

A Pipe Conveyor is used, whose enclosed design prevents the volatile material with the environment and enables a low-noise transport. This was of particular significance in this project as the conveyor runs over roads, rails and residential areas. In the residential areas, a particularly noise-reduced idler design developed by BEUMER is used, which meets the high noise protection requirements in this area. The prescribed limit of 35 decibels at a distance of ten metres from the conveyor roughly corresponds to a very quiet room fan at low speed. Here, the system also achieves a slope of 23 degrees, which can be easily implemented with a Pipe Conveyor. Because of the rough terrain, special cranes and even helicopters were used during the installation.

THE INDIVIDUALLY FITTING SYSTEM

How does the system provider manage to provide the appropriate solution for each of these applications? "We can draw on our comprehensive experience," says Martin Rewer, team lead overland conveyor at BEUMER Group. BEUMER Group installed the first conveyor of this type with horizontal curves already in 1969; the first downhill conveyor with regenerative drive in 1980. Since the 1990s, BEUMER Group has also developed into one of the leading suppliers of Pipe Conveyors. In 2019, two systems were commissioned in China that, with 5,500 tonnes of iron ore per hour, defined the current performance peak of the globally installed systems of this technology.

Since the first overland conveyor with horizontal curves was constructed in 1969, components such as idlers, belts and drives have continued to develop. In addition, the systems are becoming larger and longer and the routes more complex. This resulted in the necessity to also constantly improve the calculation and the planning tools in order to not only withstand the requirements, but to even be one step ahead.

In the first step of project planning, the systems must be dimensioned for the respective task. Using BEUMER calculation programs, a team of experts calculates the existing motion resistances and the related static and dynamic tractive forces of the belt of the system. These on the other hand determine both the drive power to be installed and the belt strength, and are also considered in the dimensioning of the horizontal curves.

"The energy consumption of long, horizontal belt conveyors is determined by the main resistance in the upper and return strand in stationary operating conditions," describes Rewer. The energy consumption consists of the running resistance of the idlers, the indentation rolling resistance and the flexing resistance of both the conveyed material and the belt when running over the idlers. The forces required for overcoming these resistances depend on various operational and design parameters. They can be determined with the so-called single resistance method. If components with low running resistances are considered, such as belts with reduced indentation rolling resistance or running-optimised idlers, the calculations of the systems nowadays show considerably lower tractive forces of the belt than a few years ago. This not only results in lower energy costs. Since the tractive forces of the belt are at a lower level, also the radii of the horizontal curves can be selected to be correspondingly smaller, because these forces are decisive for the design of these curves. Accordingly, the routing of overland conveyors can now be realised in a more flexible way and with smaller radii.

FROM THE VIRTUAL TOOLBOX

"In order to plan the conveyor for the individual application, we reach into our virtual tool box," Rewer explains. "This way we can arrange the whole routing of the system and then discuss it with the customer as a 3D plan". BOLT, the BEUMER Overland Layouting Tool developed specifically for this purpose, generates almost automatically a digital 3D model of the conveyor in the virtual landscape during the project planning. The required topography data are available in the public domain or are provided by the customer. Often drones are used. The aerial photographs include topographical information, which is then processed into digital terrain models.

In the simulation environment, the experts can adapt the conveyor to the route. The almost real illustration of the conveyor in the landscape also serves to recognise possible obstacles and to consider them accordingly in the project planning. Furthermore, the technicians are able to add the earthworks (cut & fill) and the steelwork structures in simple and precise way and evaluate them. BOLT not only ensures a very fast first project planning of the route. Especially modifications or adaptations during the project can be taken into account within short time. Project-critical data can be supplied at short term by BOLT. It includes the definition of the entire equipments on the route as well as the coordinates for foundation and earthworks. Since these data are generated automatically and updated by BOLT in case of modifications, possible required adaptations of the route are not further time-critical. All necessary data can be generated immediately after rescheduling.

"With this procedure we are able to considerably accelerate the project planning," promises Christoph Dorra. "We have the possibility to provide the customer in advance with a concrete 3D project planning, which can be easily modified during the project life. This procedure allows us to tighten the time frame for the project".

"Vertical Approach" in deep-sea mining

Seafloor massive sulfides are a valuable mineral raw material found at the bottom of the deep sea. The "Vertical Approach" is a method for extracting seafloor massive sulfides using the trench cutter method, an established technique in specialist foundation engineering that is operated and supported in the deep-sea environment from a ship on the open sea. As a relatively small-scale intervention with a minimal ecological footprint, this approach is an ideal method for test mining and exploration of deposits up to a depth of 3,000 m.

The approach was conceived in discussions between BAUER Maschinen GmbH and the Harren & Partner Group concerning opportunities to combine the expertise of both companies and to develop new strategies for sustainable mining approaches in accordance with the standards of the International Seabed Authority (ISA).

On August 26, a joint venture agreement was signed between the two companies and Seabed Mineral Services GmbH was established. The first stage is to determine the economic viability and, in particular, the environmental compatibility of the "Vertical Approach."

"We are thrilled to have found an expert partner in Bauer who is willing – just like us – to seize opportunities and take on a pioneering role in the field of deep-sea mining. Our joint approach for this venture is based on a combination of established technologies. This enables us to minimise the technological risk while at the same time keeping costs down," says Heiko Felderhoff, Managing Director of Harren & Partner.

Leonhard Weixler, head of the Diaphragm Wall Equipment division at BAUER Maschinen GmbH, adds: "The chemistry between us is very good; we share a similar spirit. This partnership is an ideal union of specialist knowledge and experience in the afield of offshore technologies and services with expertise in the development and production of specialist foundation engineering equipment for onshore and offshore customers around the world."

Heiko Felderhoff and Leonhard Weixler act as Managing Directors of Seabed Mineral Services GmbH.

The concept behind the "Vertical Approach"

Deep-sea sampling undeniably has an impact on sensitive deep-sea ecosystems. Nevertheless, the "Vertical Approach" makes the utmost effort to minimise the ecological footprint. A serious concern when it comes to deep-sea mining is the stirring up of sediment and the potential impact on sensitive deep-sea species. To prevent fine material from escaping the cutting area, a protective collar is positioned around the cutting wheels at the start and the actual cutting process is protected by the surrounding ore. As a result, fine material from the cutting process remains within this area, while the water mixed with fine sediment and cutting chips is pumped into the ore container.

The separation process is carried out within the ore container to separate the particles from the sea water via sedimentation. After this treatment, the water is fed back to the cutting wheels and reused in the cutting circuit. This closed system minimises the volume of sea water that is impacted by the cutting process.

Sampling is selective: the template and trench cutter are lowered using a cable winch instead of being initially positioned then moved horizontally along the seafloor. This restricts the sphere of influence to the base area of the template feet and trench cutter. Zones with ore can be clearly separated from zones without ore.

Another aspect of the "Vertical Approach" that reduces the environmental impact of this method compared to other methods is that only one "tool" is used for extracting material. The soil does not need to be crushed later for transport to the ship. Only the raw material is extracted, with minimal impact on the environment.

Schaft project PEA deems $2.6bn copper mine viable

Canadian resource company Copper Fox Metals has published a promising preliminary economic assessment (PEA) of the Schaft Creek copper/molybdenum/gold/silver deposit, in British Columbia.

The project covers 55 779 ha of mineral concessions and is located 60 km south of Telegraph Creek, near existing transportation and energy infrastructure.

The Schaft Creek project, which is managed through a joint venture between fellow Canadian miner Teck Resources as 75% owner and operator and Copper Fox as 25% owner, has an after-tax net present value of $842-million and an internal rate of return of 12.9%.

The PEA envisions that the project can generate yearly earnings before interest, taxes, depreciation and amortisation of almost $700-million, at full production, for the first five years and $10.8-billion of earnings for the duration of the 21-year mine life.

The project could also produce about 5-billion pounds, or 2.3-million tonnes, of copper, 3.7-million ounces of gold, 16-million ounces of silver in concentrate and 226-million pounds of molybdenum.

In the first five years of full operation, the Schaft project has the potential to produce, on average, 398-million copper equivalent pounds a year.

Schaft Creek could be constructed for an initial capital cost of $2.6-billion, while sustaining capital cost could range at $848-million.

Copper Fox CEO and president Elmer Stewart says the operator can now consider a C$23-million work programme to advance the project to prefeasibility stage.

ABEL supplies two HMQ pumps for International Mining Industry

ABEL continues to strengthen its global presence in the mining sector. The latest additions to this market are orders for two HMQ pumps (Hydraulic Quadruplex Diaphragm Pump) received the Northern German pump manufacturer from Peru and Macedonia.

One HMQ pump will be used to transport tailings in a mine in Peru at 4600 masl, which is a big challenge that ABEL will overcome. Our customer is planning on increasing production to achieve the market requirements and they have trusted on ABEL HMQ reliability for that purpose on the tailing management facility.

Our customer in Macedonia has decided to make a big step forward on the tailings management by constructing a new Paste Plant on site that will serve to avoid the usage of the tailing dam. With this process on duty (>75% solid content), natural environment is strictly respected and safe. ABEL HMQ will serve as a key partner of the paste plant to backfill the underground stopes while the mine keeps advancing at a faster pace.

These two orders specially reinforce ABEL image on the tailing management: thickened tailings transport, backfilling, and dry stacking.

The robust design, ease of operation, high availability and low maintenance, and proven track record of more than 110 installations worldwide for various combinations of highly concentrated ash slurry (fly ash + bottom ash, salt water) make ABEL reciprocating diaphragm pumps the preferred choice for pumping abrasive slurry in various industries.

ABEL HMQ pump.

ABB technology to improve quality and lower production costs for Tata Steel plant in India

Global technology company ABB will provide electromagnetic brake systems (EMBR) for two compact strip production (CSP) casters at Tata Steel's flagship plant in Jamshedpur, India, working under contract from engineering and construction organization SMS Group.

Jamshedpur, located in the eastern state of Jharkhand, is India's first planned industrial city and was established following the founding of Tata Iron and Steel Company by Jamsetji Tata and his son Dorabji Tata in the 1900s.

ABB's scope of supply also includes DCS800 DC drives, dry type transformers, water cooling systems, commissioning services and metallurgical performance evaluation. ABB is contracted through SMS which specialises in plant construction and mechanical engineering for the steel and nonferrous metals industry.

The contract builds on ABB's large installed base with premier steel producers globally. ABB EMBR is installed on 40% of thin slab casting strands worldwide and allows for higher quality and faster throughput. This well-established technology, invented by ABB in 1985, enables steelmakers to achieve steel cleanliness similar to conventional vertical bending casters, improves casting speed and increases mold copper plate lifetime. By generating a static magnetic field, which decreases meniscus metal flow speed and turbulence, the ABB EMBR provides a whole range of metallurgical improvements including elimination of mold powder entrapments, a more even molten mold powder layer and a meniscus which is flatter, hotter and less turbulent.

"The project at Tata Steel in Jamshedpur is a key order for ABB," said Raghu Badrinathan, Area Sales Manager – ABB Metallurgy. "It builds on our large installed base with premier steel producers around the world."

"Tata Steel is a highly-valued customer for ABB and it is our continuous endeavor to provide the best-in-class technology and solutions to them," said Vipul Gautam, Group Vice President, Global Account Executive for Tata Group, ABB. "We believe that our metallurgy solutions and particularly the ABB EMBR solution will help them to achieve superior performance of their casters in minimum time, lowering their cost of production while improving quality."

Reducing fire risk

The global mining industry is pivotal to the world's economy, with industries across the globe depending on the supply of commodities from underground. In its search for, extraction, beneficiation, and processing of naturally occurring solid minerals from the earth, mining is an industry that relies on plant machinery to do the heavy lifting.

Some of the biggest trucks on the planet are found working tirelessly at mines and can move extreme payloads more than 450 tonnes, which is more than a fully loaded Airbus A380. With multiple diesel engines generating 6 times more power than a Formula 1 racing car, these trucks operate around the clock in extreme conditions. Along with dozers, excavators, wheel loaders and shovels, these heavy lifters are relied on to keep these operations moving 24 hours a day.

Fire poses an ever-present threat to mine operations, with over a third of fires originating from vehicles. A small fire in a mine, either on the surface or underground, can rapidly become catastrophic result in loss of life. Heat, flammable fluids, and rapid air flow in engine bays culminate to provide a near perfect environment for fires to start.

Mining regulations can be complex and can differ significantly from country-to-country. But an unquestionable parallel is the approach to reducing fire risk. Which is why regulators,

Fire spread in a coal mine will depend upon the thermal and physical properties of the most abundant fuel sources (including coal, wooden mine roof supports, and conveyor belts), the mine's ventilation system, and the size of the mine opening[1]. Because fuel sources are typically distributed throughout a mine, a fire can spread quickly over large lateral distances. Moreover, mine fires can be especially perilous because the toxic fire products can quickly spread far beyond the fire zone and thereby expose all underground miners to dangerous and deadly conditions.

The leading causes of US mine fires include flame cutting and welding operations, frictional heating and ignitions, electrical shorts, mobile equipment malfunctions, and spontaneous combustion[2]. The fact that mine fires continue to occur emphasises the importance of recognising and eliminating potential fire hazards and the overall need for improved fire control and suppression technology. The NIOSH mine fire research program is addressing a broad spectrum of problem areas facing the US mining industry. The intent of the work is to provide the mining industry with an understanding of the conditions that could lead to a fire, the capability to detect unusual heating or fire conditions, and the technology to suppress and extinguish a fire. Work under this research program includes testing, evaluating, improving, and modifying coal mine fire-fighting strategies and methodologies through large-scale tests. One portion of this work is focused on understanding the characteristics of mine fire combustion products and flame spread through deep-seated fire experiments and use of CFD modelling.

In 2001, NIOSH and MSHA agreed to partner in research studies to develop new understandings of the characteristics of mine fires and the capabilities and limitations of mine fire suppression technologies. Since that time, NIOSH researchers and MSHA technical specialists have worked together in the field at actual mine fire sites and in the laboratory and each have gained new insights into the science of mine fires and fire control and suppression technology. This study represents the second stage of a series of deep-seated fire tests. The first study examined the combustion characteristics of wood crib blocks and direct application of fire suppression agents[3]. Future work will concentrate on large-scale deep-seated coal fires in an underground setting followed by remote application of fire suppression agents. It is anticipated that these experiments combined with follow-up CFD modelling work will provide significant information about combustion products and flame spread rates and will assist in furthering our understanding of the evolution and growth of a mine fire.

OBJECTIVE AND APPROACH

The objective of this study was to conduct two deep-seated fire experiments, including a coal fire and a mixed fuel fire (coal and wood cribbing blocks combined), to collect combustion product information, measure flame spread rates and to study the mechanics of the fire through computer modelling.

NIOSH FIRE SUPPRESSION FACILITY

The fire tests were conducted at the NIOSH Fire Suppression Facility (FSF) and MSHA provided supplemental gas monitoring equipment for the tests along with technical experts to operate the equipment. The FSF is part of the NIOSH Lake Lynn Laboratory (LLL) which is located approximately 60 miles southeast of Pittsburgh, Pennsylvania. The LLL is a world-class, highly sophisticated surface and underground facility where large-scale explosion trials and mine fire research work is conducted[4].

The FSF was configured to simulate a 150-ft long mine entry. The interior height of the simulated entry is 7.2 ft, and the width is 18 ft. The roof of the simulated entry is made of corrugated steel bridge planks, the ribs are made of 8-in thick mortared solid concrete blocks and the floor is made of reinforced concrete. The interior roof is covered with a 2-in thick layer of Fendolite M-II ® (a specialised fire-resistant mixture of vermiculite and Portland cement) and a 1-in thick layer of Fendolite MII® has been placed on the ribs.1 For ventilation, a 6-ft diameter variable speed axivane fan (equipped with a pneumatic controller to adjust fan blade pitch) was installed at one end of the simulated entry. The fan can provide blowing sustained airflow up to about 1150 fpm over the cross-section of the entry. Two doors, which permit access to the inside of the FSF, are located about 47 ft from the fan. **Figure 1** shows the exterior of the FSF.

The FSF is equipped with an array of chromel-alumel thermocouples (type-K) projecting 1.2-in down from the mine roof. The thermocouples are spaced at 10-ft intervals starting about 10 ft from the fan leading along the centreline to the end of the simulated entry. The thermocouples are connected via a wire network to a computer-based data acquisition system. During the fire tests, temperature data was collected at 10-second intervals. Radiation corrections were not made in the temperature data.

The components of the fire gases were measured using a 9-point gas sampling array located 20 ft from the trailing edge of the burn box used to contain the fires. The array consisted of an interconnected network of ½-in diameter black iron pipe set across the width of the mine entry. A total of nine, 1/8-in diameter holes were drilled into vertical sections of the pipe to sample the fire gases. The holes in the pipe were spaced equally apart from the roof-to-floor and across the width of the entry. A thermocouple was also positioned at each gas sampling point to measure the temperature of the fire gases. The gases collected at each sample point were mixed in a manifold that penetrated the FSF roof. The manifold was connected to a tubing line that led to the NIOSH and MSHA gas analysis equipment.

The NIOSH infrared gas analyser's measured oxygen (O_2), carbon monoxide (CO) and carbon dioxide (CO_2) gas concentrations and the resultant data were collected at 10-second intervals and recorded by a computer-based data acquisition system. In addition, gas samples were collected periodically over 3- to 4-minute intervals from the gas sampling array and were analysed using gas chromatography. Chromatography analysis of each of the gas samples took about ten minutes to complete, therefore during each test a sample was collected and analysed approximately every 13-15 minutes. The gases analysed included hydrogen (H_2), O_2, CO, CO_2, methane (CH_4), acetylene (C_2H_2), ethylene (C_2H_4), and ethane (C_2H_6). The NIOSH and MSHA gas analysers and the MSHA gas chromatograph were calibrated before each test. After each test, the MSHA gas analysers were checked with fresh air to determine instrument drift.

Figure 1: Fire Suppression Facility.

GAS AND FIRE MONITORING (PART 1)

damage to the FSF floor. The sides, back, and bottom of the box were constructed of expanded metal and 1 in angle iron was used as the frame (the front and top of the box was left open). The box was equipped with 16 chromel-alumel thermocouples (type-K) projecting 8 in inward from the sides. The thermocouples were spaced at 4-in and then 8-in intervals starting from the front of the box and leading towards the back of the box. The alignment of the thermocouples formed two layers of 8 units and simultaneously formed four rows of 4 units. This arrangement permitted researchers to construct 3-dimensional views of the fires. The thermocouples were connected via a wire network to the computer-based data acquisition system mentioned previously.

COMPOSITION OF THE COAL AND WOOD

The coal used in each test was mined from the Pittsburgh Coalbed. The coal was cleaned and sorted (mostly 2-in sized pieces) and was stored outside for about 6 months. Two coal samples were collected for laboratory analyses, including ultimate, proximate, and heating value determination. The wooden cribbing blocks were comprised of a variety of mixed hardwood species including ash, cherry, maple, white and red oak, and poplar. The blocks were 14 to 20 months old and had been stored underground at the LLL for about a year prior to the tests. Ten crib blocks (each block measured 6 in high, by 8 in wide by 16 in long) were randomly collected and 3-in cube-shaped samples were cut from each of the selected crib blocks and were sent to an independent testing laboratory for moisture, ultimate analysis, and heating value determinations. The averaged laboratory data for the coal and wood crib samples are shown in Table 1.

DEEP SEATED FIRE TESTS

A 3-ft-long by 2-ft-wide by 1-ft-deep box was constructed to hold the coal and wood during the fire tests. Legs (6 in) were attached to elevate the box and prevent heat

The fires were initiated using a natural gas burner that was equipped with 60 stainless steel jets (with a rated heat output of 44 to 114 kW). The burner was tilted on an angle upward toward the box to evenly spread flame across the opened front of the box. Natural gas was used instead of an accelerant (e.g., diesel fuel) to assist in starting the fires because it was more readily consumed by the fire and left no residue that could have altered the combustion products. It was arbitrarily decided to operate the burners for 45 to 60 minutes to ensure that the fires would burn without the need to re-light the burners. A steel plate was placed over the burners on an angle away from the fan across the front of the box creating an air deflector. This deflector was necessary to keep the fires burning. **Figure 2** shows the position of the box in the FSF.

Prior to igniting the fires, the ventilation flow rate was measured in front of the burn box and at the gas sampling array. At each location, the ventilation air flow rate was measured at nine points in the cross-sectional area of the mine entry and an average flow rate was determined. **Table 2** shows the averaged ventilation air flow rate data for the tests. It should be noted that the ventilation flow rate

Table 1: Averaged laboratory data from coal and crib block samples.

Parameter	Coal			Wood		
Sample Condition	AR[1]	Dry	DAF[2]	AR	Dry	DAF
Moisture, pct	8.90	–	–	14.95	–	–
Proximate Analysis						
Ash	7.23	7.94	–	0.68	0.79	–
Volatile Mattr	33.73	37.02	40.21	72.54	85.27	85.95
Fixed Carbon	50.15	55.05	59.80	11.85	13.94	14.05
Ultimate Analysid						
Hydrogen	5.67	5.14	5.58	6.39	5.54	5.59
Carbon	68.63	75.34	81.83	42.21	49.63	50.03
Nitrogen	1.26	1.38	1.50	0.16	0.19	0.19
Sulfur	0.66	0.72	0.79	0.12	0.14	0.14
Oxygen	16.56	9.50	10.32	50.44	43.71	44.06
Ash	7.23	7.94	–	0.68	0.79	–
Heating value, Btu/lb	12,202	13,394	14,549	7,184	8,446	8,513

1, As Receivd
2, Dry ash-Free

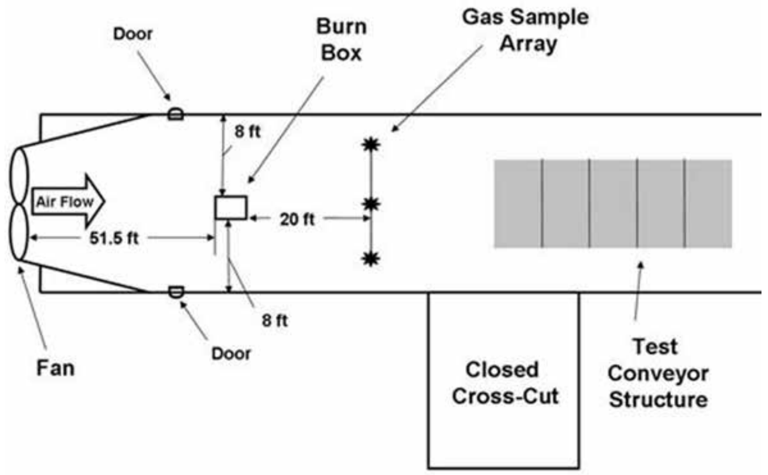

Figure 2: Layout sketch of the FSF for the deep seated fire tests.

Table 2: Average ventilation flow rate information for the fire tests.

Test No.	1	2
Ventilation flow rate in front of burn box, ft/min.	160	350
Ventilation flow rate at the gas sampling array, ft/min.	150	300

for Test 2 was more than double that of Test 1 because fan problems precluded a sustainable lower flow rate.

DEEP SEATED FIRE TEST 1

As mentioned previously, two deep-seated fire tests were conducted in this study. The first involved 202.5 lbs of coal. The coal was placed into the burn box so that the leading edge of the pile facing the fan measured 4 in deep. The pile was tapered upward towards the back of the box and reached its maximum depth of 8 in at the midpoint of the box. Two layers of 8 thermocouples were placed

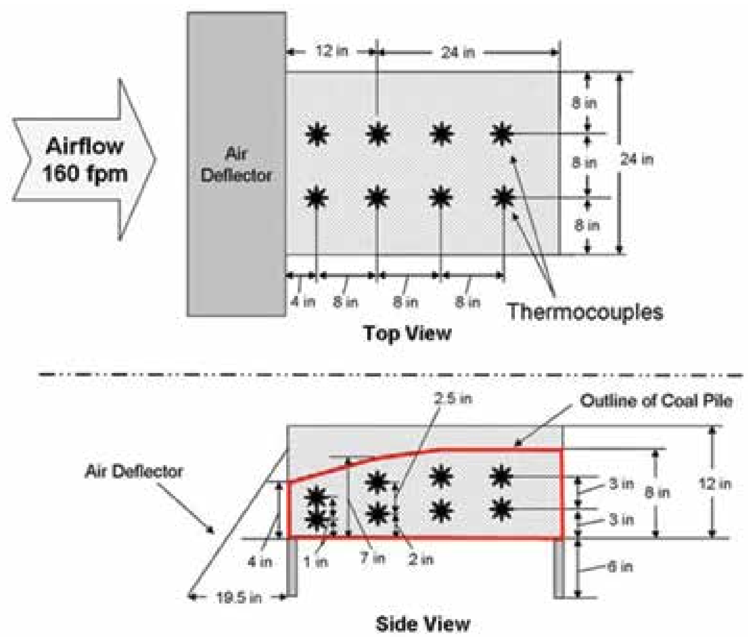

Figure 3: Airflow, layout of the coal and thermocouple array for Test 1.

in the pile. The top layer was positioned below the surface of the coal and the bottom layer was positioned above the expanded metal surface. **Figure 3** shows two views of the box and location of the thermocouples. **Figure 4** shows a picture of the box just prior to igniting the burner.

After the burner was turned off (after 45 minutes of elapsed time), it was observed that the leading edge of the fire was burning intensely. This burning condition was needed to ensure that the fire would burn to completion. During the test, the collected gas samples showed only CO and CO_2 were detected in the air stream and the concentration of these gases was below the lower reliable limit of detection. This was most likely since the fire was small relative to the size of the FSF and the ventilation flow rate. Therefore, this data could not be used to calculate the heat release rate of the fire. The fire burned slowly from the front to back in 70.5 hrs and reached a maximum temperature of 788°C. **Figure 5** shows the time-temperature traces from the thermocouples for the test. The figure presents four vertical slices through the coal pile at 4-, 12-, 20-, and 28in (measured from the leading edge of the box) and shows the progression of the fire at these positions over time.

The varied shape of the temperature plots from Test 1 are believed to be caused, in some cases, by burning coal falling away from a thermocouple resulting in a temperature decline and in other cases from burning coal falling onto a thermocouple causing the temperature to increase or be sustained for a longer period.

A pyrolysis temperature of 525°C was used in this study and when the temperature at a thermocouple reached this value, the flame front was considered to have reached that location[5]. The average flame spread rate of this fire was calculated to be 1.1 in/hr. This is a slower rate than those measured by Smith (1.9 and 2.1 in/hr) for a set of similarly sized coal fires[6]. Also, in the previous work conducted by Smith, the ventilation flow rate was 380 + 20 ft/min as compared to 160 ft/min used in this test which could account for some portion of the difference in the flame spread rates[6].

As mentioned earlier, 202.5 lb of coal was consumed in 70.5 hrs yielding a mass-loss rate of 2.9 lb/hr. Using the heating value of 13,394 Btu/lb from **Table 1**, the mass-loss rate converts to a heat release rate of 650 Btu/min (11.4 kW). The amount ash remaining after Test 1 was 8.8% which was only slightly higher than the 7.2% average value shown in **Table 1**, indicating that most if not all the coal was consumed in the fire.

DEEP SEATED FIRE TEST 2

As described previously, the material used for this fire was a blend of the two most common fuel sources found in a coal mine, namely coal and wooden cribbing blocks. The wood crib blocks were cut into two sizes to fit the scale of the box. The larger cut size blocks measured 2.8 in by 2.5 in by 22 in and the smaller cut blocks measured 2.8 in by 2.5 in by 7.9 in. A total of 7 large and 9 small blocks were used in this test and the blocks consisted of a mix of the various hardwoods

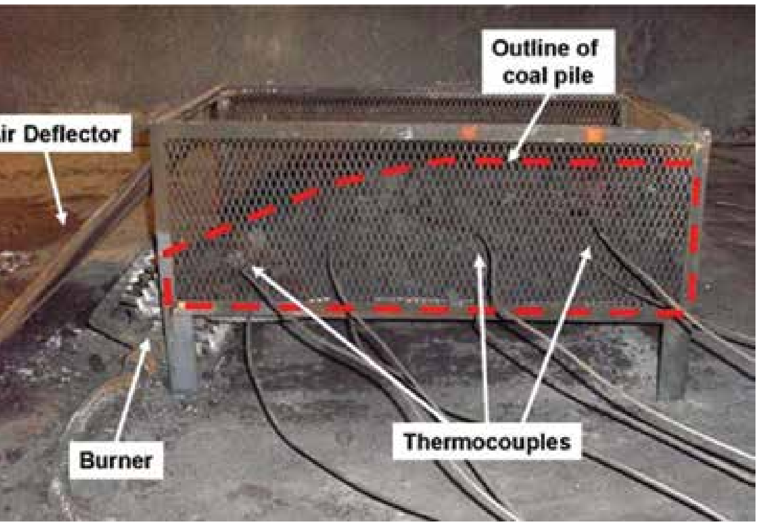

Figure 4: Side view of box just prior to Test 1.

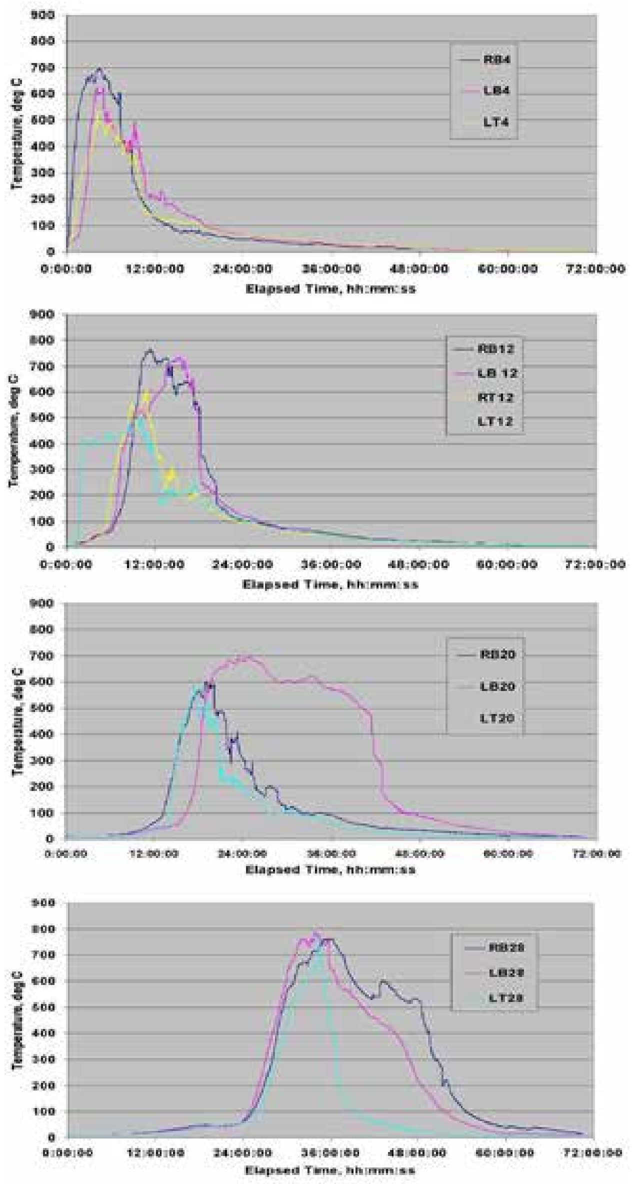

Figure 5: Time-temperature traces from thermocouples for Test 1. The terms RB, LB, RT, and LT refers to the right bottom, left bottom, right top and left top respectively. Note data from RT4, RT20 and RT28 was omitted due because of instrument failure.

described previously. A row of blocks (3 large and 3 small) was placed into the burn box with the long axis of the blocks parallel to the long axis of the box. Coal was placed into the box to fill the spaces between the blocks. A second row of 4 large blocks was placed perpendicular to the first row. Again, coal was used to fill in the open space between the blocks. The top row of blocks was formed by placing 6 small blocks perpendicular to the previous row and coal was used to fill in the open spaces. A total of 170 lbs of coal and 42.8 lbs of wood were used in this test.

The wood and coal mixture were placed in the burn box so that the leading edge facing the fan measured 6 in deep. The mixture was tapered upward towards the back of the box and at the midpoint reached a maximum depth of 8 in. As in Test 1, two layers of 8 thermocouples were used. The top layer of thermocouples was positioned above the second row of wood and the bottom layer was positioned above the lowest level of wood. **Figure 6** shows two views of the box and location of the thermocouples for the test. **Figure 7** shows a picture of the box just prior to igniting the burner.

The ventilation air was increased by almost 100% for this test because there were problems maintaining a sustained airflow at lower flow rates. The burner was turned off after 60 minutes and the fire was observed to be burning intensely. As in the previous test, the collected gas samples showed that the concentration of the combustion products in the air stream were below the lower reliable limit of detection. This was again most likely since the fire was small relative to the size of the FSF and the ventilation flow rate. Therefore, this data could not be used to calculate the heat release rate of the fire. **Figure 8** shows (as in the previous test) time-temperature traces from the thermocouples and presents four vertical slices through the coal and wood mixture at 4-, 12-, 20-, and 28-in from the leading edge of the box. The figure illustrates the progression of the fire at these positions over time.

As in Test 1, the varied shape of the temperature plots from Test 2 are believed to be caused, in some cases, by burning material falling away from a thermocouple resulting in a temperature decline and in other cases from burning material falling onto a thermocouple causing the temperature to increase or be sustained for a longer period.

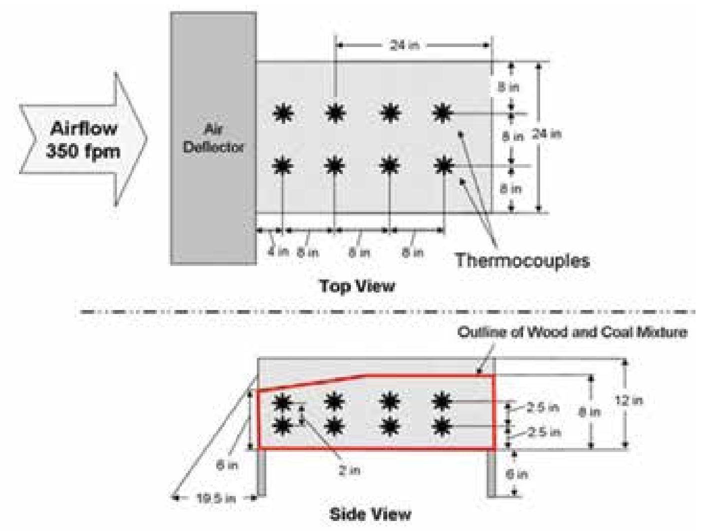

Figure 6: Airflow, layout of the coal and thermocouple array for Test 2.

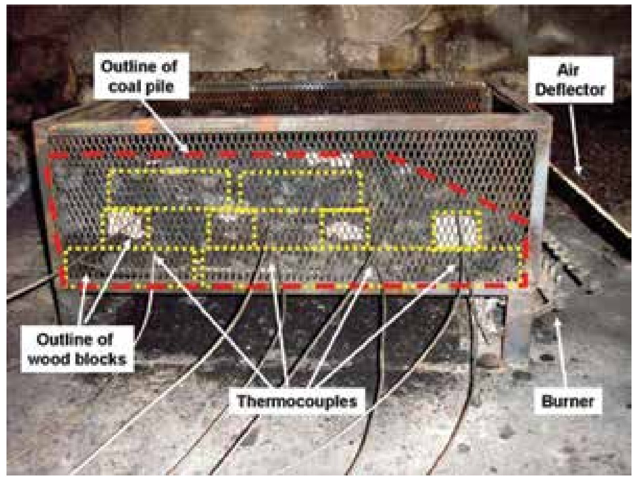

Figure 7: Side view of box as configured for Test 2.

The mixed fuel fire burned faster than the coal fire and was completed in about 36 hrs. The maximum observed temperature of this fire was 1163°C. As in Test 1, the flame spread rate of the fire was measured when the temperature of the fire was reached 525°C at a thermocouple location. The average flame spread rate was calculated to be 2.0 in/hr (about 82% faster than the coal fire in Test 1). Again, this faster rate can be attributed to the increased ventilation flow rate and the fact that the wood most likely burned at a faster rate than the coal.

As mentioned previously, 170 lb of coal was consumed in 36 hrs yielding a mass-loss rate of 4.7 lb/hr. Using the heating value of 13,394 Btu/lb from Table 1, the mass-loss converts to a heat release rate of 1050 Btu/min (18.4 kW). This fire also consumed 42.8 lbs of wood yielding a mass-loss rate of 1.2 lb/hr. Using the heating value of 8,446 Btu/lb from **Table 1**, the mass-loss converts to a heat release rate of 170 Btu/min (3.0 kW) producing a combined heat release rate for the fire of 1220 Btu/min (21.4 kW). The amount ash remaining after Test 2 was 7.2% which was only slightly higher than the 5.9% value calculated from the coal and wood ash data shown in **Table 1**, indicating that most if not all the coal and wood was consumed in the fire.

CFD MODELLING OF FLAME SPREAD FOR THE COAL FIRE

Flame spread in the coal fire was simulated using Fire Dynamics Simulator (FDS), a computational fluid dynamics (CFD) program developed by National Institute of Standards and Technology. Because of its very complicated geometry, no attempt was made to simulate the mixed fuel fire. FDS is a three-dimensional, large eddy simulation model developed to study the transport of smoke and hot gases during a fire in an enclosed space. FDS is the most widely used large eddy simulation model in the fire science field and has demonstrated good agreement with experimental data in numerous validation studies. The model uses finite difference techniques to solve the Navier-Stokes equations numerically for fluid flow with a mixture fraction combustion model. Most mine combustibles undergo combustion by a gas phase reaction of the volatiles generated by the pyrolysis of the material. The pyrolysis front advances as a reaction front into the solid fuel leaving behind a char layer[1]. The FDS includes a pyrolysis model.

Figure 9 shows the physical model of the coal pile, the burner, and the FSF. The dimensions for the model FSF

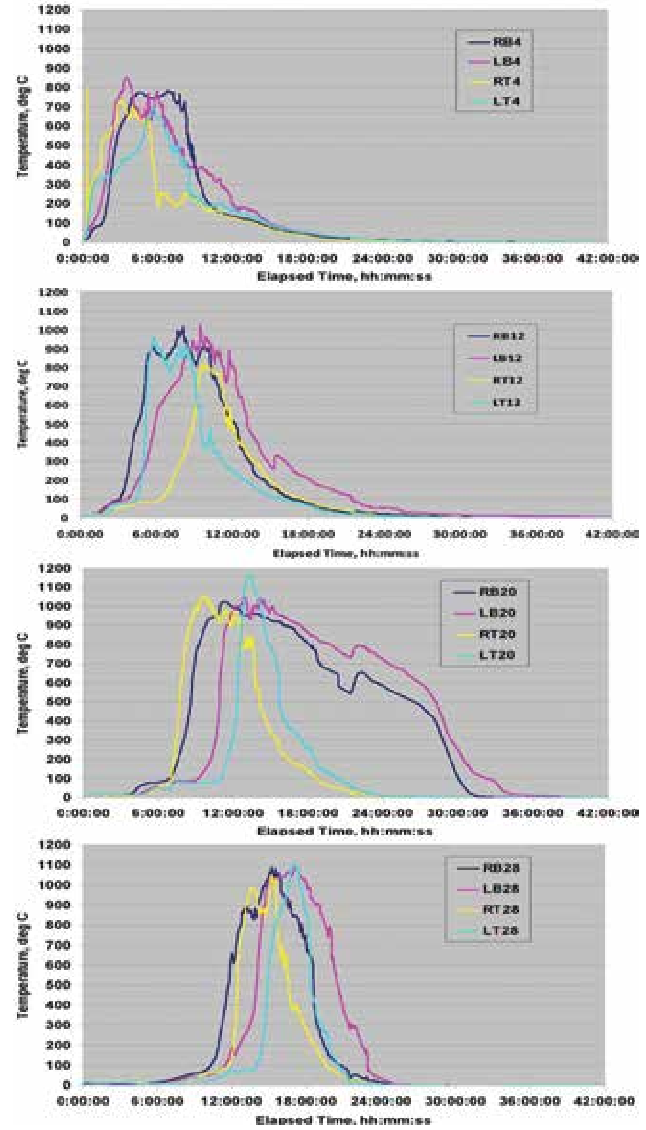

Figure 8: Time-temperature traces from the thermocouples for Test 2.

were 18 ft wide by 7.2 ft high (the same as the actual FSF). For the simulation the length of the FSF was limited to 19.7 ft. The coal was modelled as a rectangular volume with dimensions of 3 ft long by 2 ft wide by 8 in high. The burner was modelled using its average heat release rate of 81 kW. In the simulation, the burner was kept on for 50 minutes. The airflow velocity at the inlet of the model FSF was 157 fpm like Test 1. Eight surface thermocouples were created in the simulation and were designated as T1 to T8. The thermocouples were in the top of the pile like those in Test 1. Thermocouples T1 and T5 were located at the 4 in position, T2 and T6 were at 12 in position, T3 and T7 were at the 20 in position and T4 and T8 were at the 28 in position (as measured from the leading edge of the box).

In the simulation, the coal was treated as a continuous-medium with constant physical properties. The coal density was 1330 kg/m^3; coal specific heat was 1.05 kJ/kg-K; coal conductivity was 0.24 W/m-K; and the heat of combustion for the coal was 13,460 Btu/lb. In the simulation, the pyrolysis front advances with an endothermic heat of reaction. The heat of pyrolysis was 209 kJ/kg, and the pyrolysis temperature of the coal was 525°C[5].

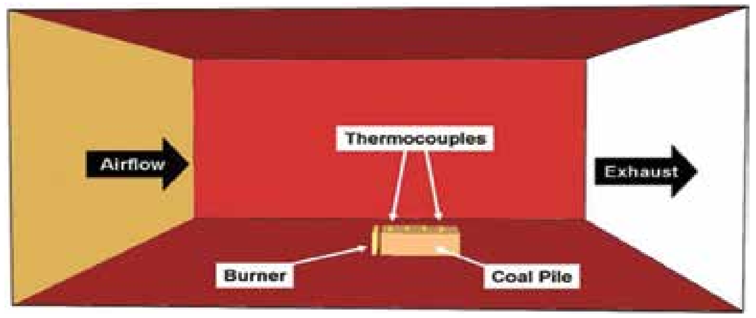

Figure 9: The physical model of coal pile, burner and the simulated FSF.

Figure 10 shows temperatures at different thermocouple locations as calculated in the simulation. Only temperatures at thermocouples T1-4 are presented. As mentioned previously, the varied shape of the temperature plots from Test 1 are believed to be caused, in some cases, by burning coal falling away from a thermocouple resulting in a temperature decline and in other cases from burning coal falling onto a thermocouple causing the temperature to increase or be sustained for a longer period. In the simulation however, this could not be duplicated because the coal was treated as a continuous medium and as such the temperature plots do not fall off quickly as observed in Test 1. It can be seen from the figure, the surface temperature increased slowly at the beginning except for thermocouple T1 which increased quickly because it was close to the ignition burner. This stage is a typical pre-heating period. After reaching about 450°C, the temperature increased very quickly to 700°C, indicating the arrival of the flame. The flame spread rate was 2.1 in/hr from T1 to T2, 2.9 in/hr from T2 to T3 and 3.1 in/hr from T3 to T4.

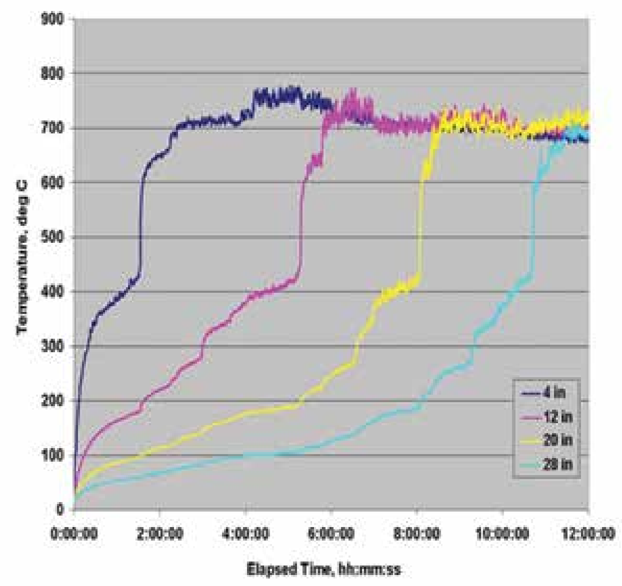

Figure 10: Time-temperature traces from the thermocouples for the CFD coal fire simulation.

DISCUSSION

Figure 11 shows time-average temperature traces for thermocouples at each location for both tests. The plots were constructed by determining the average temperature for all thermocouples at each position (4-, 12-, 20-, and 28-in from the leading edge of the box) over the life of the test. The plot shows how differently these fires behaved. The coal fire burned slower and at a lower average temperature while, the mixed fuel fire burned faster and was significantly hotter than the coal fire. Part of the difference between the two tests can be attributed to the fact that the wood components in Test 2 were not evenly sized relative to the coal pieces. This difference was considered in the design of the experiment, and it was decided that the larger wood pieces more closely approximated that found in a coal mine. Given that the wood burned at a faster rate than the coal, the flame front would also move faster through the coal and wood mixture. Also, some of the difference between the two fires can be attributed to the variation in ventilation air speed. A CFD analysis by Edwards and Hwang showed that the flame spread rate in a simulated coal lined tunnel was strongly sensitive to ventilation air speed[1]. Further experimentation is warranted to identify the exact relationship between flame spread and ventilation air speed.

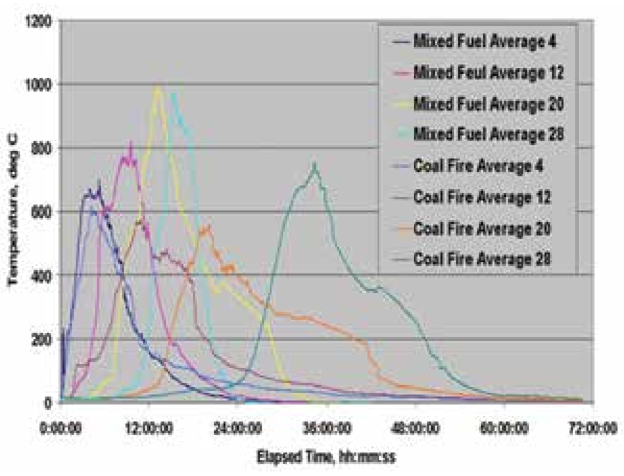

Figure 11: Time-average temperature plots at each position for Tests 1 and 2.

Table 3 shows a comparison of the parameters from Test 1 with the FDS simulation of the coal fire. Compared to Test 1, the maximum surface temperatures as estimated in the simulation are very close to those measured in the test. However, the simulation overestimated the flame spread rates. This is probably because the coal pile was treated as a continuous medium in the simulation, while in Test 1 it consisted of packed pieces of coal. With the continuous medium, heat conduction is stronger than in packed coal pieces leading to higher flame spread rate.

Table 3: Comparison of Test 1 data to FDS simulation.

Parameter	Test 1	FDS
Ventilation rate, fpm	160	157
Average flame spread rate, in/hr	1.1	2.7
Maximum temperature, °C	788	777

SUMMARY

In this study, two, deep-seated fire tests including a coal fire and a mixed fuel fire (coal and wood combined), were conducted in partnership with MSHA at the NIOSH Fire Suppression Facility to collect combustion product information, measure flame spread rates, and to study the mechanics of the fire through computer modelling. These tests are part of a large-scale fire test program that is ongoing at the NIOSH Lake Lynn Laboratory. Unfortunately, because of the small size of the fire tests, relative to the FSF, we were unable to collect meaningful fire combustion product information.

A comparison of the two fire tests showed that the fires behaved differently with the coal fire burning more slowly and achieved a lower temperature than the mixed fuel fire. Part of the difference can be attributed to the fact that the wood components in Test 2 were not evenly sized relative to the coal pieces. This difference was considered in the design of the experiment, and it was decided that the larger wood pieces more closely approximated that found in a coal mine. Given that the wood burned at a faster rate than the coal, the flame front would also move faster through the coal and wood mixture. Additionally, the difference in the ventilation flow rates between the two tests undoubtedly contributed to the rate of flame spread (1.1 in/hr with a ventilation flow rate of 160 ft/min for the coal fire test versus 2.0 in/hr with a ventilation flow rate of 350 ft/min for the mixed fuel fire test).

CFD modelling of the Test 1 showed the maximum surface temperatures in the simulation were very close to those measured in the test. But the flame spread rates from the simulation are higher than those estimated in the test. This is probably because that the coal pile was treated as a continuous medium in the simulation, while in Test 1 it consisted of packed pieces of coal. The results from this modelling exercise will be used in the design of the follow-up large-scale underground deep seated coal fire experiments with remote fire suppression applications.

ACKNOWLEDGMENTS

The authors would like to recognise Melanie D. Calhoun and Edward J. Arnold, MSHA, Richard A. Thomas, John Soles, NIOSH, and the NIOSH staff at the LLL, for their professionalism, dedication, and assistance in the conduct of the field work for this study. We would also like to recognise Thomas A. Gray, Tetra Tech, and Charles R. Wiedrich, MSHA for their expertise in providing the technical review of this paper.

REFERENCES

1. Edwards, J.C., and C.C. Hwang, 2006. CFD Modelling of fire spread along combustibles in a mine entry. In: SME Annual Meeting and Exhibit. Preprint 06-027. Littleton, CO: Society for Mining, Metallurgy, and Exploration, Inc., pp. 1–5.
2. National Institute for Occupational Safety and Health, 2008. NIOSH Mining Webpage, <http://www.cdc.gov/niosh/mining/topics/topicpage1
9. htm>, November 26.
3. Trevits M.A., A.C. Smith, J.E. Urosek, M.P. Valoski, 2007. Evaluation of deep-seated crib block fires and direct-application fire suppression agents. In: SME Annual Meeting and Exhibit. Preprint 07-130. Littleton, CO: Society for Mining, Metallurgy, and Exploration, Inc., pp. 1–14.
4. National Institute for Occupational Safety and Health, 1999. "Lake Lynn Laboratory (flyer)," Pittsburgh, PA: US Department of Health and Human Services, Public Health Service, Centres for Disease Control and Prevention, National Institute for Occupational Safety and Health, Publication No. 99149, 1 p.
5. Hertzberg, M., I.A. Zlochower and J.C. Edwards, 1988. Coal particle pyrolysis mechanisms and temperatures, US Bureau of Mines Report of Investigation 9169, 39 p.
6. Smith, A.C., D. Ng, W. Ryan, C.P. Lazzara, 1991. A method to evaluate the performance of coal fire extinguishers, US Bureau of Mines Report of Investigations 9392, 11 p.

Advancements in underground gas testing

An underground mining operation proves to be a risky venture as far as the safety and health of workers are concerned. These risks are due to different techniques used for extracting different minerals. The deeper the mine, the greater is the risk. These safety issues are of grave concern especially in case of coal industries. Thus, safety of workers should always be of major consideration in any form of mining, whether it is coal or any other minerals. Underground coal mining involves a higher risk than open pit mining due to the problems of ventilation and potential for collapse. However, the utilization of heavy machinery and the methods performed during excavations result into safety risks in all types of mining. Modern mines often implement several safety procedures, education and training for workers, health, and safety standards, which lead to substantial improvements in safety, level both in opencast and underground mining.

A worker in a mine should be able to work under conditions which are safe and healthy for his body. At the same time the environmental conditions should be such as will not impair his working efficiency. This is possible if mine air is nearly the same as on the surface without toxic and inflammable gases.

The gases are the present in the underground mines are flammable gas (CH_4), Noxious gases (NO_2, NO_3, N_2O_5), Carbon Monoxide (CO), Carbon Dioxide (CO_2). Hydrogen Sulphide (H_2S), Sulphur Dioxide (SO_2). The permissible limit set for these gases are as follows:

- Underground air should not have more than 0.5% CO_2 or other noxious gases.
- Inflammable gas should be below 0.75% in the general body of return air and below 1.25% at any place in the mine.
- The general air on road must not normally contain more than 0.005% of CO[1].

Table 4: (In this table the sources and the explosives limits of the common gases that are found in the mine are shown)[4]

Name	Primary sources in mines	Hazards	Flammability limits in air (%)
Methane (CH4)	Strata	Explosive, Breathing problem	5 to 15
Carbon dioxide (CO2)	Oxidation of carbon, fires, explosions	Increased heart rate and breathing	N/A
Carbon monoxide (CO)	Fires, Explosions, blasting, incomplete combustion of carbon compounds	Highly toxic, Explosive	12.5 to 74.2
Sulphur dioxide (SO2)	Oxidation of Sulphides, acid water on sulphide ores	Toxic, irritant to eyes, Throat, and lungs	N/A
Nitrogen dioxide (NO2)	IC engines, blasting, fumes, welding	Toxic, Throat and lung infections	N/A
Hydrogen Sulphide (H2S)	Acid water on sulphides, Strata decomposition of organic materials	Highly Toxic, irritant to eyes and explosive	4.3 to 45.5

Different gases that are present in the mine have different effects on the human body and can also cause explosion if reaches above a certain limit. The effects of some of the harmful gases are as follows:

- Carbon Dioxide on 3% (breathing gets doubled), 6% (headache, exhaustion), 15 %(consciousness loss), 25% (death after hours).
- Carbon Monoxide on 0.02 %(headache, discomfort), 0.12 %(palpitations after 10 minutes of work), 0.2% (unconsciousness after 10 minutes of work), 0.5%-1.0% (death after 10-15 minutes of work).
- Methane This is the gas which is responsible for most of the underground mine explosions. It forms a layer just below the roof of the mine. The gas is not poisonous but can suffocate a person due to lack of oxygen[2].

ADVANCEMENTS IN UNDERGROUND GAS TESTING

Detection by warm blooded birds

In the earlier days for the gas detection the warm-blooded birds like munia were commonly used as they as they are affected much earlier than man by CO. such birds form essential equipment for the rescue party entering the mines after an explosion or fire. With 0.15% of CO present in the air a bird shows distress (ruffing of feathers, pronounced chirping and loss of liveliness) in 3 minutes and fall of the perch in 18 minutes. With 0.3% CO the bird shows almost immediate distress and fall of its perch in 2-3 minutes. Immediate signs of distress are not likely to be observed on birds when exposed to only 0.1% CO.

Coal has always been the primary resource of energy in India, which has significantly contributed to the rapid industrial development of the country. About 70% of the power generation is dependent on it. Thus, the importance of coal in energy sector is indispensable. But the production brings with it the other by-products, which proves to be a potential threat to the environment and the people associated with it. Present work is a sincere attempt in analysing the graveness and designing a Gas Monitoring system of detection by using the Zigbee technology.

A wired communication system inside underground mines is not effective, efficient, economic, and reliable. Due to unexpected roof fall at any moment the entire communication system of the total network may collapse.

Effective communication is critical to the success of response and rescue operations; however, unreliable operation of communication systems in high-stress environments is a significant obstacle to achieving this. To improve security, protection and productivity in underground mines, a consistent communication system must be established between personnel, working in the premises of underground mine, and the control room. A wireless communication system is must for the safety point of view of the personal working inside the underground mines. Therefore, a fast, accurate, flexible, and reliable Zigbee Wireless network technology is used in our work[3].

The key issue of research on wireless sensor networks is to balance the energy costs across the whole network


Munia bird as a part of search rescue team of a mine.


Dragger multigas detector.

MQ4

and to enhance the robustness to extend the survival time of the whole sensor network. Zigbee technology is given preference over others such as Wi-Fi for the establishing of wireless network because it provides a large range of coverage and less fluctuation in the signals.

Colour charting detectors

These types of detectors are filled with some chemicals and changes the colour according to the concentration of a particular gas present in the atmosphere. Later the colour of the tube is matched with the chart and the percentage of the harmful gases can be determined. Eg P.S detector, Hoolamite detector, Drager-multigas detector.

Automatic fire damp detector

Automatic fire damp detector

Many companies have now started producing automatic detectors which tells the exact concentration of the gases present in the mine environment, these devices are able to detect even a very small amount of gas percentage. some of the leading companies that manufactures these kinds of devices are EMCOR, M.S.A Ltd. , Uptron etc. these gas detecting devices are also featured with adjustable probe to take the readings from the roof. Eg Automatic fire damp detector, Interference Methanometer, memacs I etc.

Gas detecting sensors

These sensors are used in the chemical plants to detect the gas leakages. These sensors have now started to find application in the underground mines for the continuous monitoring of the harmful gases. Eg MQ4, MQ7.

COMPONENTS OF THE WIRELESS NETWORK THIS MONITORING SYSTEM CONTAINS SEVERAL COMPONENTS LIKE

boards (Arduino board and Zigbee USB interfacing board), LCD (Liquid crystal display), different sensors and other small electronic components.

Arduino UNO

The Arduino board is a specially designed circuit board for programming and prototyping with Atmel microcontrollers. The microcontroller on the board is programmed using the Arduino Programming Language (based on Wiring) and the Arduino development environment (based on Processing). It is relatively cheap and plug straight to computers USB port or power it with an AC-to-DC adapter or battery to get started[5].

Zigbee USB Interfacing Board

Zigbee (Xbee) USB Interfacing Board is used to interface Xbee wireless module with computer systems. This Board is used to connect Zigbee modules to make communication between PC to PC or laptop, PC to Mechanical Assembly or robot, PC to embedded and microcontroller-based Circuits.

Table 5: Famous mine disasters due to gas leaks

S.no.	Date	Place of Accident	Cause of Accident	Fatalities
1.	Sep 6, 2006	Nagda incline of Bhatdih colliery, BCCL, India	Explosion in the mines due to the accumulation of methane	50 miners were declared dead
2.	Feb 22, 2009	Tunlan, Underground coal mine, Northern China	Poor ventilation responsible for the accumulation of the methane gas	77 miners were dead and 114 were hospitalise ed
3.	Oct 28, 2013	Underground coal mine, North Western area, Spain	Accumulation of methane gas	6 miners have been recorder dead

Arduino UNO Board

As Zigbee communicates through Serial Communication so other end of USB, which is connected to a PC, treated as COM port for Serial Communication. It is provided with indication LEDs for ease[6].

Figure 17: Zigbee USB interfacing Board

Carbon Monoxide Sensor (MQ7)

Various types of sensors are available in the market in which semiconductor sensors are considered to have fast response. MQ7 semiconductor sensor is mainly used for detecting carbon monoxide (CO).

Carbon mono-oxide sensor

MQ-7 gas sensor composed of micro Al_2O_3 ceramic tube and Tin Dioxide (SnO_2). Electrode and heater are fixed into a crust. The heater provides required work conditions for the work of sensitive components. The conductivity of sensor is higher along with the gas concentration rising. When the sensor, heated by 5V it reaches at high temperature, it cleans the other gases adsorbed under low temperature. The MQ-7 have 6 pins in which 4 of them are used to fetch signals and other 2 are used for providing heating current[7].

MQ-4 Sensor and MQ-4 Module

Methane Gas Sensor (MQ4)

MQ-4 gas sensor composed of ceramic tube and Tin Dioxide. Electrode and heater are fixed into a layer. The heater provides required work conditions for the work of sensitive components.

When the target combustible gas present, the conductivity of sensor is higher along with the gas concentration rising. The MQ-4 sensor has 6 pins in which 4 of them are used to fetch signals and other 2 are used for providing heating current[8].

SYSTEM ARCHITECTURE

This monitoring system mainly consists of two units. First one is Sensor Unit another one is Monitoring unit.
Sensor unit contains two parts:

Display Unit (A)

Transmitter Unit (B)

Display unit consist of the Arduino board, sensors, and the LCD. The transmitter unit consists of a router and the sensors.

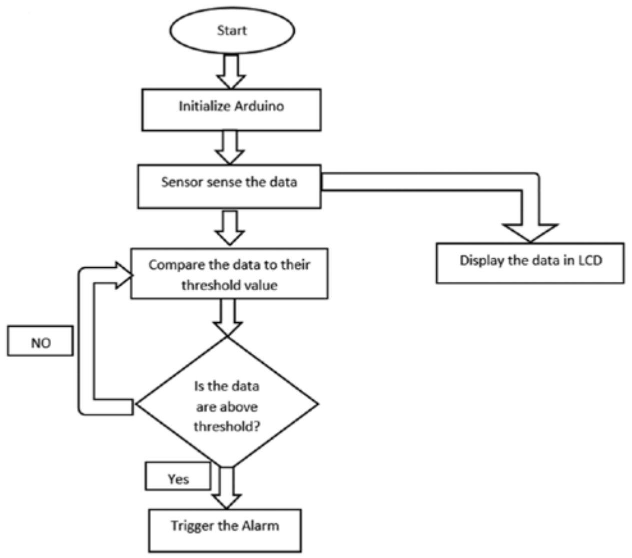

Flow chart of the monitoring System for Sensor Unit: (A)

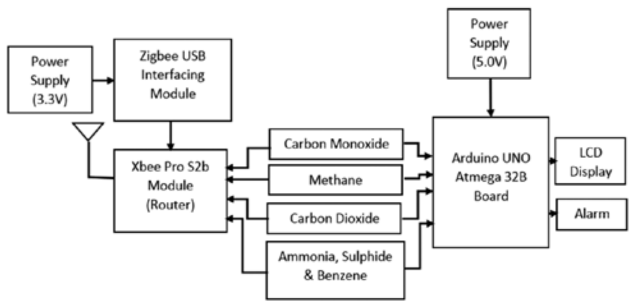

Block diagram of Sensor Unit: (B)

GAS AND FIRE MONITORING (PART 2)

INSTALLATION ZONE

The following are the main places to install the detector:

- **Goaf area:** This is one of the main places from where gas can be leaked
- **Return airway:** The importance of return airway cannot be underestimated. It can carry enough of the hazardous gases
- **Near faults, fractures or any such geological discontinuity:** These places are also prone to gas leaks
- **Where the percentage of organic matter is high:** High percentage of organic matter means more gases. So, where coal percentage is higher than the rest, we must put the sensors.
- Near the roof to detect methane layering.
- Near the working face[9].

CONCLUSION

This paper deals with the hardware implemented for the real time monitoring system and how to proceed if the presence of any of the harmful gas have been detected. The details of each components used were described briefly based on its functionality and specifications. The flow chart and block diagram show the organization and working of the system. This system also stores all the data in the computer for future inspection.

ACKNOWLEDGMENT

The authors of this paper are very much thankful to Dr V.L.Narasimham, Dr. N.P.Nayak, Dr Santanu bhowmik and Dr D.K.Gupta for their continuous assistance until the completion of this project and express heartily gratitude to their seniors and friends for their valuable advice, resourceful guidance, and continuous inspiration throughout the preparation of this paper. The views expressed in this paper are those of the authors and not necessarily of the organization to which they belong.

REFERENCES

1. Deshmukh.D.J. (2014). Elements of Mining Technology vol 2. Nagpur: ennet.
2. http://www.buzzle.com/articles/methane-gasexposure-symptoms.html
3. Srivastava.S.K, real time monitoring system using wireless sensor network (2015).
4. Deshmukh.D.J. (2014). Elements of Mining Technology vol 2. Nagpur: ennet.
5. http://www.arduino.cc/
6. Boddu, R., Balanagu, P., Babu, N.S. (2012), Zigbee based mine safety monitoring system with GSM
7. https://www.sparkfun.com/datasheets/Sensors/Biometric/MQ-7.pdf
8. https://www.sparkfun.com/datasheets/Sensors/Biometric/MQ-4.pdf
9. Misra.G.B, (1986), Mine Environment and Ventilation. New Delhi: Oxford University Press.

Innovation and future of mining rock mechanics (Part 1)

The 121-mining method of longwall mining first proposed in England has been widely used around the world. This method requires excavation of two mining roadways and reservation of one coal pillar to mine one working face. Due to considerable excavation of roadway, the mining roadway is destroyed during coal mining. The stress concentration in the coal pillar can cause large deformation of surrounding rocks, rock bursts and other disasters, and subsequently a large volume of coal pillar resources will be wasted. To improve the coal recovery rate and reduce excavation of the mining roadway, the 111-mining method of longwall mining was proposed in the former Soviet Union based on the 121-mining method. The 111-mining method requires excavation of one mining roadway and setting one filling body to replace the coal pillar while maintaining another mining roadway to mine one working face. However, because the stress transfer structure of roadway and working face roof has not changed, the problem of stress concentration in the surrounding rocks of roadway has not been well solved. To solve the above problems, the conventional concept utilizing high-strength support to resist the mining pressure for the 121 and 111 mining methods should be updated. The idea is to utilise mining pressure and expansion characteristics of the collapsed rock mass in the goaf to automatically form roadways, avoiding roadway excavation and waste of coal pillar. Based on the basic principles of mining rock mechanics, the "equilibrium mining" theory and the "short cantilever beam" mechanical model are proposed.

Key technologies, such as roof directional presplitting technology, negative Poisson's ratio (NPR) high-prestress constant-resistance support technology, and gangue blocking support technology, are developed following the "equilibrium mining" theory. Accordingly, the 110 and N00 mining methods of an automatically formed roadway (AFR) by roof cutting and pressure releasing without pillars are proposed. The mining methods have been applied to a large number of coal mines with different overburdens, coal seam thicknesses, roof types and gases in China, realizing the integrated mode of coal mining and roadway retaining. On this basis, in view of the complex geological conditions and intelligent mining demand of coal mines, an n intelligent and unmanned development direction of the "equilibrium mining" method is prospected.

Coal is an important source for energy consumption around the world, accounting for 27% of the global primary energy consumption in 2019. In China, coal consumption accounts for 57% of the primary energy consumption in 2019 (National Statistical Bureau of China, 2020). For coal extraction, the coal mining methods include short wall and longwall mining methods. The longwall mining method has been widely used due to its high productivity and good ventilation.

The 121-mining method belonging to longwall mining method (gob-side entry driving with coal pillar) was first proposed in England in 1706. The 121-mining method represents mining one working face, excavating two mining roadways, and reserving one protective coal pillar. Two mining roadways are used for coal transportation and ventilation of the working face (working face I). The coal pillar maintains the stability of the mining roadway of the next working face (working face II). A schematic diagram of the 121-mining method is shown in **Figure 1**. The 121-mining method has been widely used in coal mining, but it has the following drawbacks:

1. Considerable roadway excavation is required. Approximately 13,000 km of roadways are excavated in China each year, with significant excavation cost. In addition, it is easy to cause in equilibrium between coal mining and roadway excavation. Moreover, the excavation process mostly focuses on artificial construction, which restricts the development of intelligent and unmanned coal mines.
2. The collapsed gob roof can easily compress the coal pillar of the roadway, resulting in stress concentration at that location, which easily leads to deformation and damage to the surrounding rocks of roadway. In this method, the coal pillar reserved cannot be recovered, and a number of coal pillar resources are wasted. China's annual resource loss due to coal pillars reaches 400 x 10^6t, exceeding two hundred billion yuan.
3. The coal mining process is accompanied by significant mining pressure. Thus, highstrength support must be used in mining roadways to resist large mining pressure, which can easily cause failure of the support components and surrounding rocks of roadway. The accidents reported in the mining roadway account for 80%-90% of all coal mine accidents.
4. A broad range of goaf is formed along with coal mining. Due to coal pillar support, the fracturing and collapsing patterns of overlying strata between the goaf and coal pillar are different. The fractures continue to expand to the ground surface, leading to uneven ground surface subsidence and environmental damage. The total area of ground surface damage caused by coal mining in China is expected to be 18,000 km^2 from 1994 to 2020, with an increasing rate of seven hundred km^2 annually.

In 1937, the 111-mining method (gob-side entry retaining with filling body) was proposed in the former Soviet Union in view of coal resource waste caused by the 121-mining method. The 111-mining method means mining one working face, excavating one mining roadway, and setting one filling body to replace the coal pillar for maintaining another mining roadway, as shown in **Figure 2**. The 111-mining method abandons coal pillar, to improve coal recovery rate and reduce excavation of the mining roadway. However, there still are some problems that should be resolved, such as stress concentration in surrounding rocks of roadway and mine ecological damage, which are also reported in the 121-mining method. These problems hinder the applications of the 111-mining method.

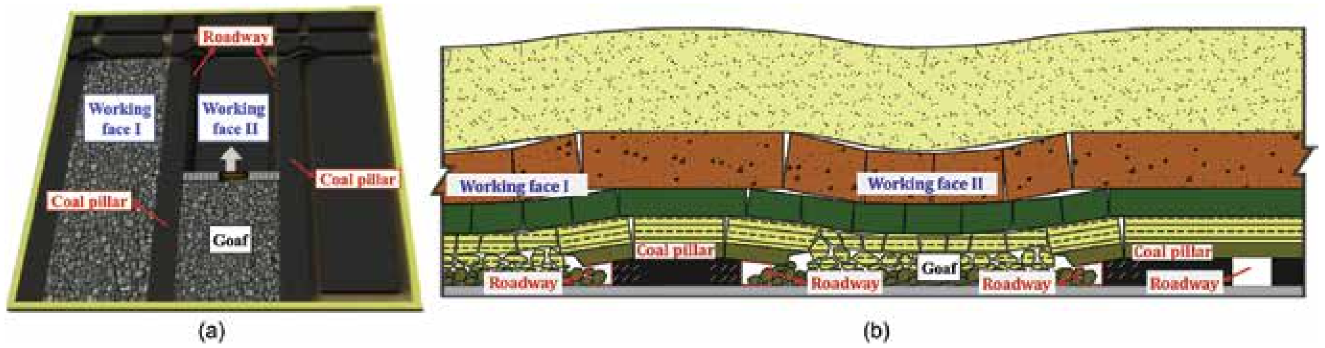

Figure 1: Diagram of the 121-mining method (UK, 1706): (a) Three-dimensional (3D) diagram of the working face; and (b) Profile of the working face.

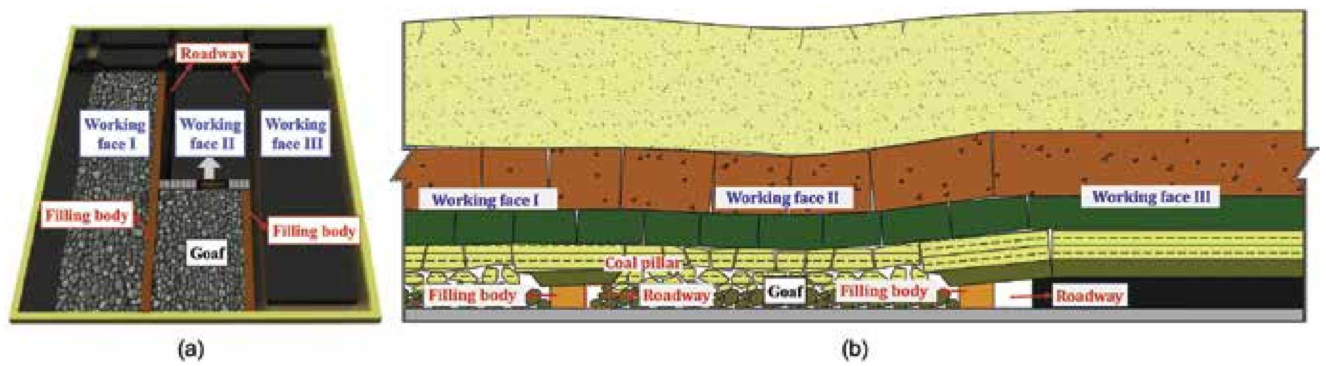

Figure 2: Diagram of the 111-mining method (former Soviet Union, 1937): (a) 3D diagram of working the face; and (b) Profile of the working face.

In view of the above-mentioned problems, extensive studies have been performed on roadway excavation, coal pillar and filling body control, roadway support, and mine ecological protection, such as "broken rock zone theory," "stress control theory", "combining support theory", "intensity weakening theory for rock burst", and "strip-filling to controlling subsidence theory". However, these theories and technologies focus on the systems utilizing high-strength support to resist the mining pressure. There is no unified research on all kinds of problems, and there are few revolutionary innovations in mining theory. As a result, it is difficult to solve the abovementioned coal mining problems from the source. The fundamental approach to solve the coal mining problems in the 121 and 111 mining methods lies in the reform of mining methods by using mining rock mechanics. Mining rock mechanics plays a significant role in reform of the coal mining method and development of mechanised intelligent equipment and technology. For this, the authors first analysed the mining pressure law of the 121-mining method in view of mining rock mechanics.

Next, the "equilibrium mining" theory was proposed, and the "short cantilever beam" mechanical model was established. Then, a new concept was proposed, which utilises the mining pressure and expansion characteristics of the collapsed rock mass in a goaf to automatically form roadways. This means that neither roadway excavation nor the coal pillar is needed. On this basis, the 110-mining method of an automatically formed roadway (AFR) by roof cutting and pressure releasing was proposed in 2009. The mining method represents mining one working face, excavating one mining roadway, without coal pillar or filling body. The stress transfer between the goaf and roadway is cut off by roof directional presplitting. The roof directional collapse and automatic roadway formation are realised through mining pressure and broken expansion characteristics of the collapsed rock mass. Based on successful application of the 110-mining method, the N00 mining method was proposed in 2016.

In the N00 method, no roadway excavation or coal pillar is needed, and the integrated mode of coal mining and roadway retaining can be realised. This lays a foundation for achieving the goal of safe, efficient, and intelligent mining.

CHARACTERISTIC ANALYSIS OF TRADITIONAL 121 MINING METHOD

Analysis of mining pressure

In the traditional 121 mining method, the mining pressure law of the working face is divided into the following five stages, as shown in **Figure 3**, and described as follows:

Stage I: before immediate roof collapse. The immediate roof consists of unstable rock strata located directly above the coal seam. The surrounding rock stress within the gob roof is re-distributed during coal mining. However, the immediate roof does not collapse in a brief period of time, with no obvious deformation of the rock strata above it (**Figure 3b**).

Stage II: immediate roof collapse. The immediate roof collapses instantly when it lags behind the working face to a certain distance under the influence of its deadweight and mining pressure. The roof collapse affects the stability of the roadway. At this stage, the gangue formed by the immediate roof collapse fails to fill the goaf, and there are no obvious fractures in the rock strata above the immediate roof (**Figure 3c**).

Stage III: main roof collapse. The main roof is stable rock strata located in the upper section of the immediate roof and can maintain a large, exposed area. Because the goaf is not filled with gangue by immediate roof collapse, the fractures of the main roof occur and the fractured roof sinks above the roadway or coal wall under the deadweight and overlying load. The caving zone forms above the goaf. Marked fractures appear in its interior structure and begin to expand to the overlying strata (**Figure 3d**). At this stage, the stress in the surrounding rocks of roadway increases due to main roof rotary extrusion. The stress concentration area appears at the roadway solid coal side.

Stage IV: fracture and subsidence of overlying strata. The main roof collapses periodically along the mining direction of the working face, with fracture and subsidence in the overlying strata. Fractures quickly expand in the overlying strata and the fractured zone forms. At this stage, the stress concentration area of the roadway solid coal side still exists, but the peak stress gradually transfers to the depth of the solid coal side (**Figure 3e**).

Stage V: ground surface subsidence. The strata above the fractured zone appear to sink after coal mining, and the sinking zone forms. Ground surface subsidence and fracture damage begin to occur as time elapses (**Figure 3f**).

Analysis of the in-equilibrium state

To understand the movement of the overlying strata and the mechanical state at various positions when applying the 121-mining method, the force characteristic of the coal pillar, movement of the overlying strata structure, and force state of the roadway support system are analysed, as shown in **Figure 4**. The analysis process is described as follows:

Force characteristic of coal pillar

Periodic collapse and fracture subsidence occur along with coal mining in the overlying strata of the goaf. The long cantilever beam structure forms above the roadway on both sides of the coal pillar. The long cantilever beam revolves and sinks to squeeze the coal pillar of the roadway, resulting in stress concentration in this area. The stress in the coal pillar is in an in-equilibrium state and cannot be released. The coal pillar can be easily crushed over time.

Movement law of overlying strata structure

Due to the coal pillar support, tensile fracturing failure gradually occurs along the strata above the coal pillar after coal mining. The fracture and collapse patterns of the overlying strata between the goaf and coal pillar are different. The overlying strata in the mining area are constantly moving and are of an in-equilibrium state. The time to reach the overall stability of the structure is significantly long. Fractures in the overlying strata gradually extend to the ground surface with time, leading to uneven ground surface subsidence and environmental damage.

Force state of roadway support system

The 121-mining method adopts high-strength support to resist mining pressure to ensure the stability of roadway.

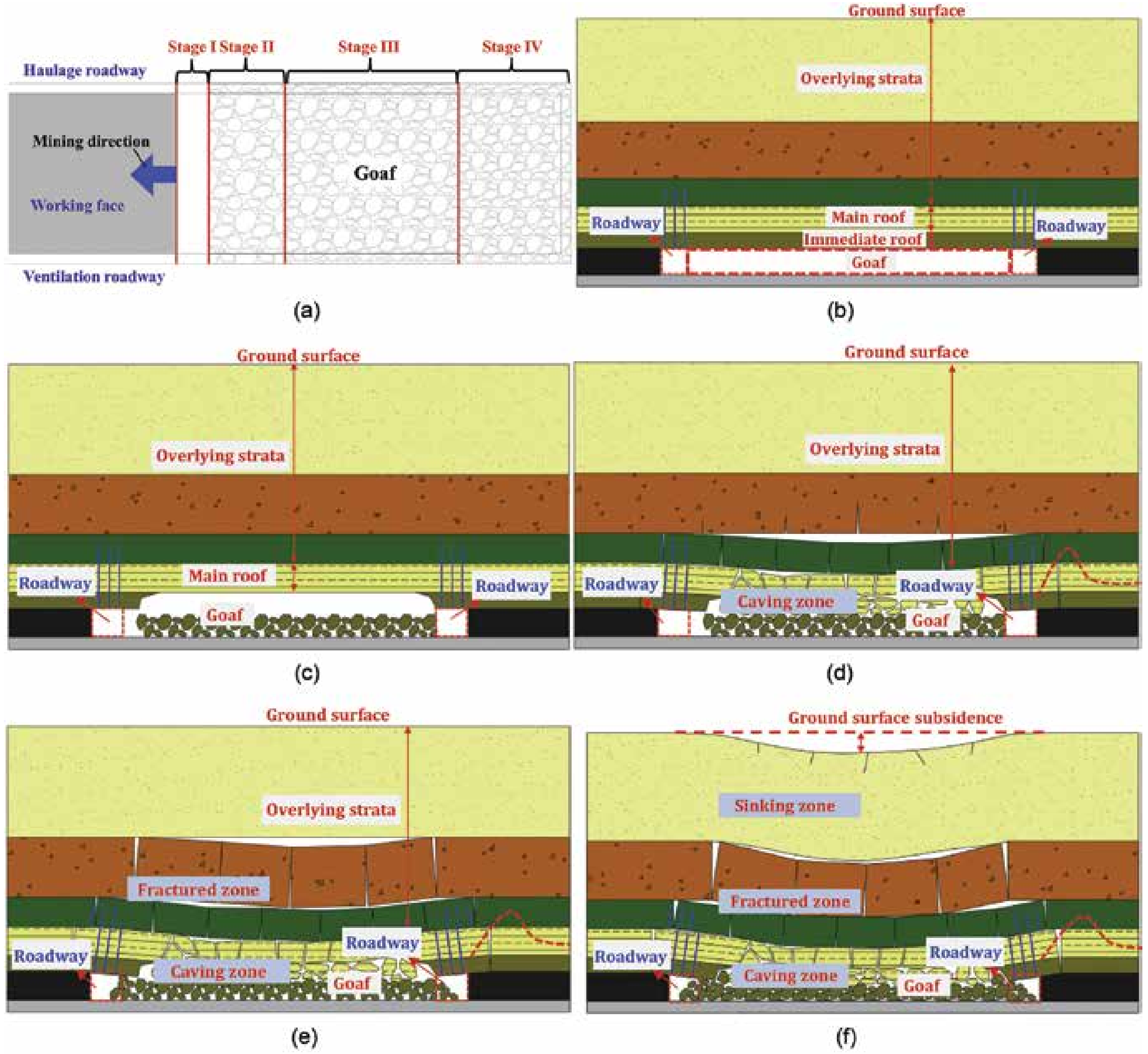

Figure 3: Schematic diagrams of mining process of the 121-mining method: (a) Plane diagram of coal mining; (b) Stage I; (c) Stage II; (d) Stage III; (e) Stage IV; and (f) Stage V.

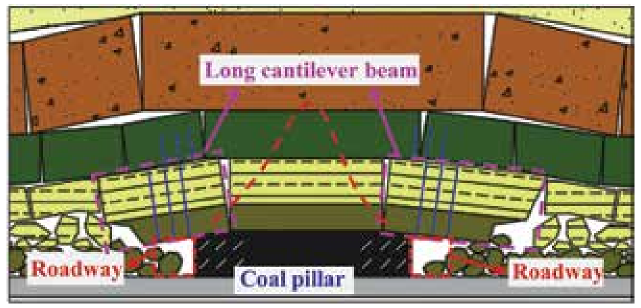

Figure 4: Diagram of the long cantilever beam structure used for the 121-mining method.

The force of the roadway support system is in an in-equilibrium state under substantial mining pressure, which is prone to causing support system failure and roadway instability.

According to the above analysis, it can be concluded that the stress in the coal pillar reserve is highly concentrated when the 121-mining method is adopted. Overlying strata structure movement above the coal pillar and two sides creates an uncoordinated and unstable state. When high-strength support is used to resist the mining pressure, the in-equilibrium force is induced in the roadway support system. Thus, the stope using the 121-mining method is in an in-equilibrium state in consideration of the force characteristic of the coal pillar, movement law of the overlying strata structure, and force state of the roadway support system.

THE "EQUILIBRIUM MINING" THEORY

The mining damage invariant equation

To understand the cause of the above "in equilibrium state" of the 121-mining method, rock strata damage at each stage of mining activity is analysed based on the mining rock mechanics. Mining activities lead to large area collapse and fracture expansion in rock strata above the goaf. Caving zone, fractured zone and sinking zone form in the roof strata, resulting in ground surface subsidence. Rock strata damage in these three zones causes

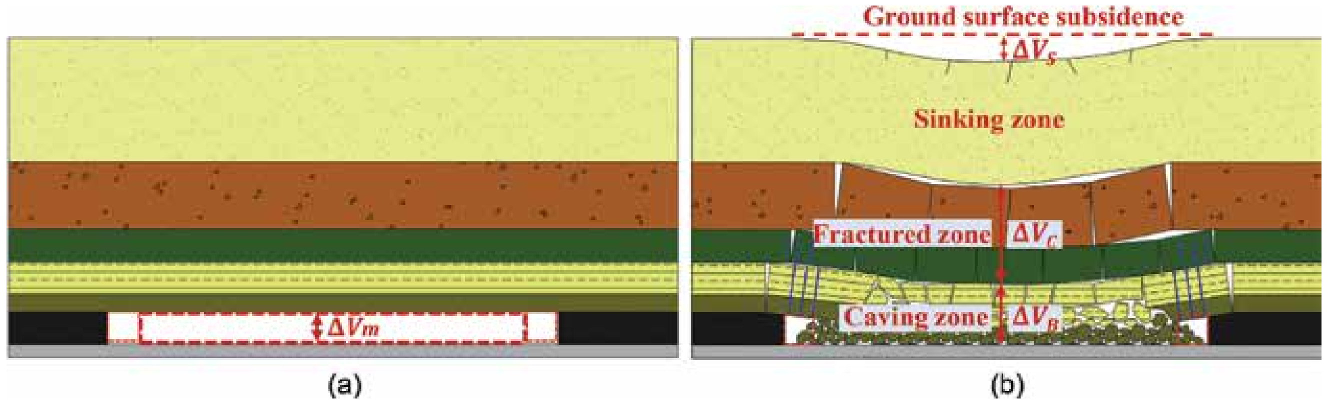

Figure 5: Rock strata damage diagram for the 121-mining method: (a) before and (b) after roof collapse.

continuous changes in the ground surface subsidence variable volume ΔV_S, the roof strata fracture increasing volume ΔV_C and the broken expansion volume of the collapsed rock mass ΔV_B. These three types of volumes are closely related to the mining volume ΔV_m in mining activities, as shown in **Figure 5**.

Combining the 121-mining method (**Figure 3**) and rock strata damage (**Figure 5**), the mining process at each stage is described as follows:

Stage I (before immediate roof collapse): $\Delta V_B = \Delta V_C = \Delta V_S = 0$.
Stage II (immediate roof collapse): $\Delta V_B < \Delta V_m$, $\Delta V_C = 0$.
Stage III (main roof collapse): ΔV_B continues to rise. At this stage, $\Delta V_B < \Delta V_m$, and ΔV_C begins to increase.
Stage IV (overlying strata fracture and subsidence): ΔV_B remains unchanged, and ΔV_C increases rapidly.
Stage V (ground surface subsidence): ΔV_S begins to increase.

Three types of rock strata damage variables are defined to describe the damage state of different rock strata. K_1 is defined as the damage variable of ground surface subsidence caused by coal mining, which is the ratio of the ground surface subsidence variable volume to the mining volume (**Equation 1**). K_2 is defined as the damage variable of roof strata fracture, which is the ratio of the roof strata increasing fracture volume to the mining volume (**Equation 2**). K_3 is defined as the damage variable of the broken expansion of the collapsed rock mass, which is the ratio of the broken expansion volume of the collapsed rock mass to the mining volume (**Equation 3**).

Equation 1 $K_1 = \Delta V_S/\Delta V_m$

Equation 2 $K_2 = \Delta V_C/\Delta V_m$

Equation 3 $K_3 = \Delta V_B/\Delta V_m$

Under different geological conditions, the above three types of rock strata damage variables constantly change. Although the changes in the three damage variables are complicated, their sum is always equal to 1. All mining engineering approaches follow this rule, which is called the invariant equation of the sum of the mining damage variables (referred to as the mining damage invariant equation):

Equation 3 $K_1+K_2+K_3 = 1$

In **Equations 1-4**, the mining volume ΔV_m of the 121-mining method is known. ΔV_S can be obtained by measurement to determine the value of K_1. However, ΔV_C and ΔV_B are not controllable, and the corresponding mining damage variables K_2 and K_3 cannot be determined. Thus, the mining damage invariant equation (**Equations 4**) of the 121-mining method cannot be solved. Combined with the in-equilibrium state analysis, the 121-mining method cannot be used for the equilibrium control of mining activities, hence this method is a typical "in equilibrium mining" system.

The broken rock mass exhibits expansion characteristics. If these characteristics can be used to realise equilibrium between the broken expansion volume of the collapsed rock mass and the mining volume, ΔV_B can be equal to ΔV_m. By substituting this value into **Equations 3** and **4**, K_3 is calculated as 1, and $K_1 = K_2 = 0$. The mining damage invariant equation (**Equation 4**) could be solved, which can be used to control the equilibrium of mining activities, forming an "equilibrium mining" system.

The model of the "short cantilever beam"

A "short cantilever beam" (He *et al.*, 2017b) model was established in 2008 for coal mining based on the above concept of "equilibrium mining", as shown in **Figure 6**. The model combines the idea of utilizing the expansion characteristics of the broken rock mass and converting the resistance to mining pressure into the utilization of mining pressure. On one hand, through directional splitting on the gob-side roof, the directional collapse of roof rock strata towards the goaf is realised by utilizing the mining pressure, and the goaf is filled with the gangue by utilizing the expansion characteristics of the gangue. Therefore, the gangue rib automatically forms in the underground space obtained during coal mining. On the other hand, gangue blocking support is used to maintain the gangue rib, and the highprestress constant-resistance anchor cable is used to control the roadway roof to ensure the stability of the surrounding rocks of roadway. The mining

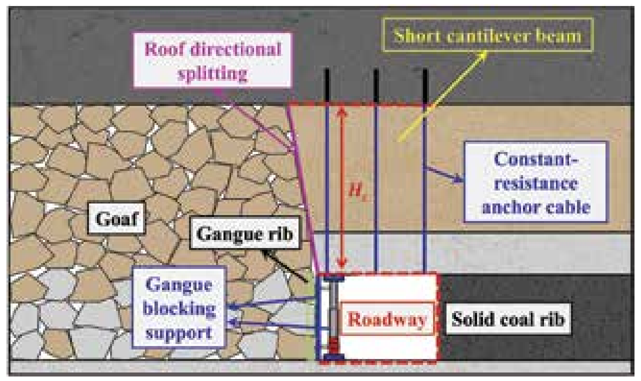

Figure 6: Model of the "short cantilever beam" for coal mining (He, 2009).

pressure and the expansion characteristics of the collapsed rock mass are utilised, and eliminations of coal pillar and roadway excavation are realised. Based on the "short cantilever beam" model, the "equilibrium mining" theory of "utilization of two aspects and elimination of two aspects" with an integrated mode of coal mining and roadway retaining is formed.

The overlying strata of the working face can collapse directionally, and the goaf can be filled with gangue using the "equilibrium mining" theory. Thus, rapid equilibrium of the overlying strata structure and the equilibrium force of the roadway support system can be realised. Based on the above theory, the mining method of AFR by roof cutting and pressure releasing without pillars (referred to as AFR without pillars) is proposed.

According to the expansion control equation of the collapsed rock mass (Equation and the equation of broken expansion (**Equation 6**) obtained from field measurement, a reasonable roof cutting height is designed to control the broken expansion volume of the collapsed rock mass. It realises equilibrium between the broken expansion volume and mining volume, where $\Delta V_B = \Delta V_m$, $\Delta V_C = 0$, and $\Delta V_S = 0$. The overall equilibrium of each roof cutting area can be realised by the above mining method, as shown in **Figure 7**.

The expansion volume ΔV_B of the collapsed rock mass of the AFR without pillars is determined by the broken expansion control equation:

Equation 5 $\Delta V_B = (K - 1)\, H_c S$

where K is the expansion coefficient of the collapsed rock mass, H_c is the height of roof splitting, and S is the area of coal mining. The parameter K can be determined from the equation of broken expansion obtained via field measurement:

Equation 6 $K = K_0 e^{-at}$

where K_0 is the initial broken expansion coefficient, α is the fitting coefficient, and t is the time.

The coefficient K varies under different rock characteristics conditions. According to the test results in the Ningtiaota coal mine in China, the curves of expansion coefficient K in different monitoring sections obtained by **Equations 6** are shown in **Figure 8**.

Characteristics of "equilibrium mining" of the AFR without pillars

The characteristics of the "equilibrium mining" system of the AFR without pillars are shown in **Figure 9**. The equilibrium state of the working face after coal mining is manifested in three aspects: automatic equilibrium of goaf, roadway equilibrium by artificial intervention, and overall equilibrium of multiple working faces, which are described as follows:

Automatic equilibrium of goaf

The overlying stratum of the goaf presents the broken expansion equilibrium during coal mining, which belongs to the automatic equilibrium state formed by utilizing the mining pressure and expansion characteristics of the collapsed rock mass. The directional splitting is carried out on the gob-side roof so that the overlying strata can collapse within the roof splitting height under its deadweight and mining

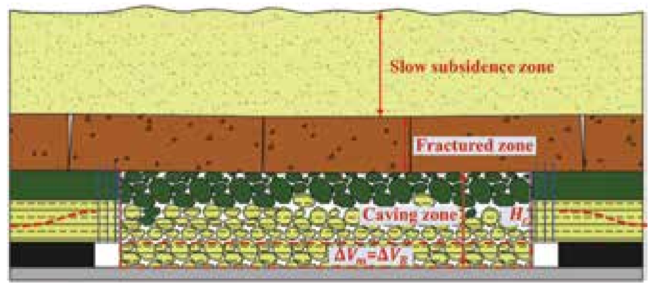

Figure 7: Analysis model of the mining damage invariant of the AFR without pillars (He, 2009).

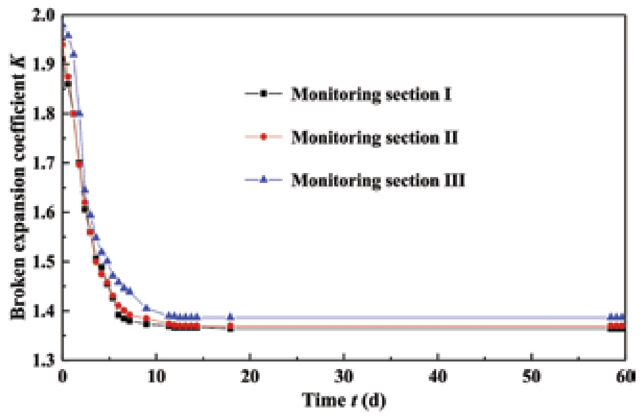

Figure 8: Curves of broken expansion coefficient K in different monitoring sections.

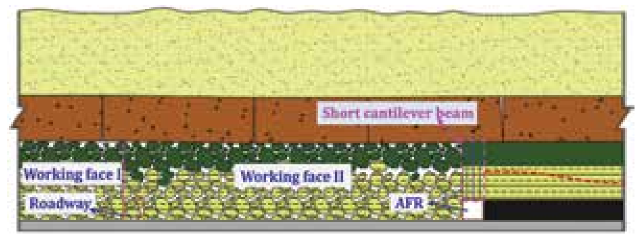

Figure 9: Mining diagram of the adjacent working face of the AFR without pillars.

pressure. The goaf is filled by continuous collapse of strata and broken expansion of gangue, which ensures that the broken expansion volume is equal to the mining volume. Therefore, goaf automatic equilibrium can be realised.

Roadway equilibrium by artificial intervention

The specific performance is as follows:

1. The structure of the "short cantilever beam" is formed under roof splitting so that the influence of gob roof movement and collapse on the roadway is reduced.
2. The collapsed rock mass in the goaf plays a certain supporting role in the "short cantilever beam" of the roadway roof based on the expansion characteristics of the collapsed rock mass.
3. The gangue blocking maintenance is carried out for the gangue rib of the roadway, and a high-prestress constant-resistance anchor cable is adopted to control the roof so that the roadway roof and the stable main roof form an integral structure. Therefore, roadway equilibrium by artificial intervention is realised.

Overall equilibrium of multiple working faces. The multiple working faces present overall equilibrium after coal mining, which avoids the influences of coal pillar and roadway

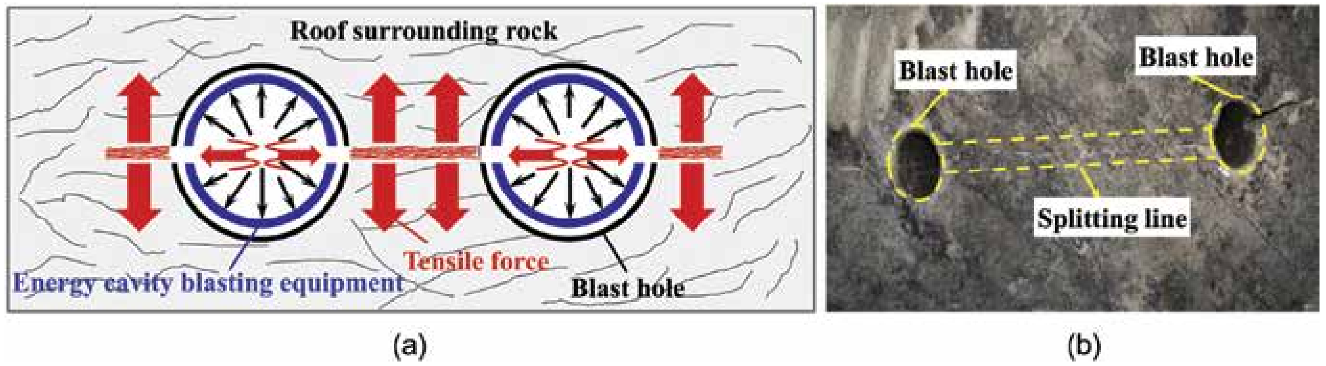

Figure 10: Bidirectional energy cavity tension blasting: (a) Technical principle; and (b) Field application (He, 2009).

excavation on working faces. The specific performance is as follows:

1. The coal pillar is eliminated. The influence of the stress concentration and the large shear force at the coal pillar are eliminated when fracturing and collapsing occur in the rock strata so that uneven ground surface subsidence is avoided.
2. The excavation of the roadway is not needed. The influence of roadway excavation in the adjacent working face (working face II) on the equilibrium area of the previous working face (working face I) can be avoided, which reduces the overall equilibrium time of the mining area. Therefore, the overall equilibrium of multiple working faces can be realised.

It is then required to develop associated key technologies based on the "equilibrium mining" theory to realise the coal mining of the AFR without pillars. To realise automatic equilibrium of goaf, roof directional splitting technology of roadways should be developed to realise roof directional collapsing and gangue filling with broken expansion. To realise roadway equilibrium by artificial intervention, high-prestress constant-resistance support technology and gangue blocking support technology should be developed to realise stable control of the roadway and equilibrium mining. Based on the above key technological developments, "equilibrium mining" technology and intelligent studies on matching equipment should be conducted to realise the unmanned overall equilibrium mining of multiple working faces.

KEY TECHNOLOGIES OF MINING METHOD OF THE AFR WITHOUT PILLARS

Three key technologies are developed based on the technical requirements of the AFR without pillars, including roof directional presplitting technology, negative Poisson's ratio (NPR) highprestress constant-resistance support technology, and gangue blocking support technology.

Roof directional presplitting technology

To control the collapsing height of the gob roof and make it collapse directionally to fill the goaf, a new presplitting technology is proposed to realise effective roof cutting. In consideration of the rock mass characteristics of high compressive strength and low tensile strength, directional presplitting technology is proposed. It consists of the bidirectional energy cavity tension blasting technique and instantaneous splitting with a single fracture surface technique.

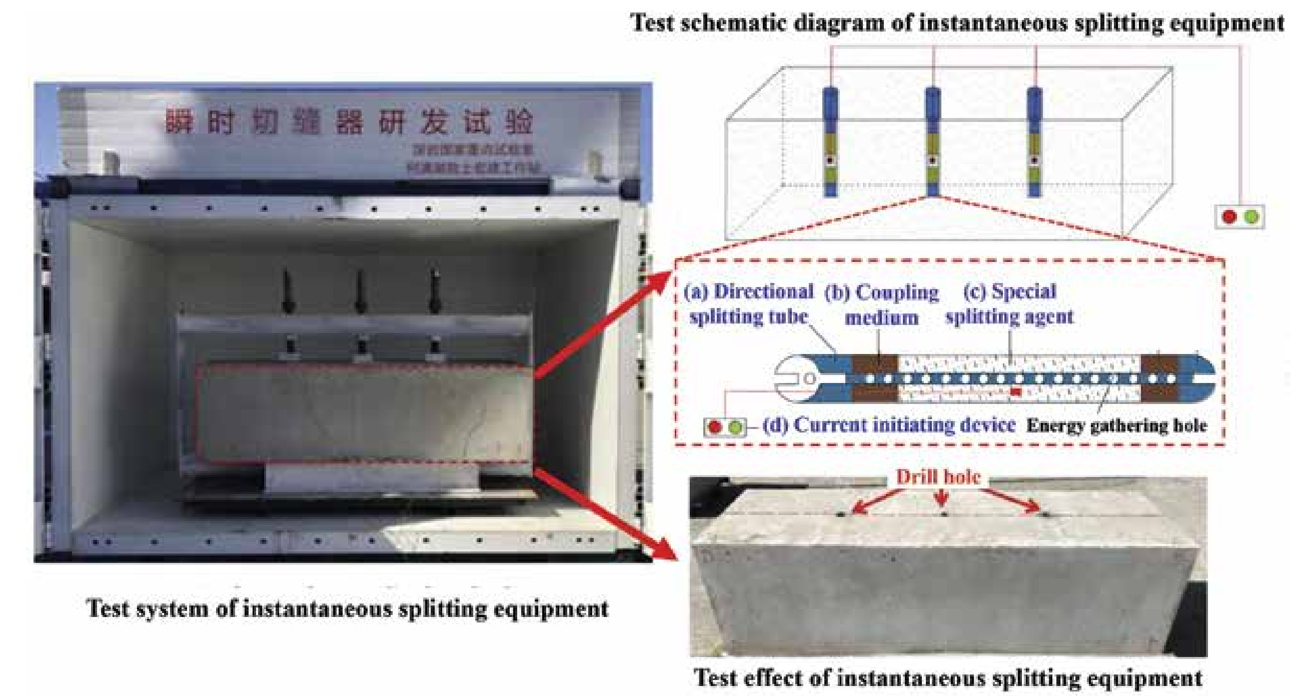

Figure 11: Laboratory test of instantaneous splitting equipment (He *et al.*, 2019).

Bidirectional energy cavity tension blasting technique

Roof directional presplitting is realised by bidirectional energy cavity tension blasting equipment (He *et al.*, 2017d; Gao *et al.*, 2019). The initial fracture is formed at the blast hole wall according to the pre-set direction when the hole is blasted. The surrounding rocks of the blast hole are uniformly compressed. The tensile stress is generated in the vertical direction of the initial fracture. The rock mass is fractured along the presplitting direction, leading to further expansion and extension of the fracture, as shown in **Figure 10a**.

Directional fractures appear along the interior and surface of the blast hole by adopting the bidirectional energy cavity tension blasting technique, with fracture rate greater than 90%. The technique can produce roof presplitting according to the pre-set position and direction, which causes the gob roof to be cut down along the presplitting line based on the design height. The field application of the technique is shown in **Figure 10b**.

Instantaneous splitting with a single fracture surface technique

Roof directional presplitting is realised by instantaneous splitting with a single fracture surface technique. It utilises instantaneous splitting equipment, which can produce a single fracture surface instantaneously without blasting and can replace the bidirectional energy cavity tension blasting technique. The new splitting equipment is composed of a (i) directional splitting tube, (ii) coupling medium, (iii) special splitting agent, and (iv) current initiating device, as shown in **Figure 11**. The coupling medium fixes the special splitting agent and transmits energy. The special splitting agent has high ignition point. When it is triggered by the current initiating device, a large amount of gas is produced in a brief period of time. The gas is discharged in the direction of the energy gathering hole at the directional splitting tube, which fractures the surrounding rocks in the direction of gas pressure.

The field test of instantaneous splitting with a single fracture surface technique is carried out in a deep coal mine (overburden of 890 m). The immediate roof of the test working face is composed of fine sandstone with an average thickness of 11.05 m and average uniaxial compressive strength of 86.3 MPa. The instantaneous splitting equipment is successful in field applications, and the fracture rate can be up to 90%, meeting the requirements of directional splitting. The field test process and effects of instantaneous splitting are shown in **Figure 12**. The indices of two kinds of roof splitting equipment applied for roof directional presplitting techniques are shown in **Table 1**.

NPR high-prestress constant-resistance support technology

The commonly used support anchor cable exhibits the Poisson's ratio (PR) effect, characterised by "local plasticity and obvious necking." Its elongation is approximately 3%-5% (Dong *et al.*, 2018), leading to poor energy absorption effect and susceptibility to failure when the deformation of the surrounding rocks is large, as shown in **Figure 13**.

During the collapsing process of the gob-side roof, large friction stress is generated on the formed "short cantilever beam" after roof directional splitting. The surrounding rocks of the roadway roof deform easily and release substantial amounts of energy. The traditional anchor cable can easily fail due to the sudden increase in stress and the PR effect, which cannot meet the control requirements of the roadway roof. To control the deformation of surrounding rocks and absorb released energy effectively, a new anchor cable must be developed. It should have good energy absorption ability and bear large deformation of the rock mass under high prestress. The NPR highprestress constant-resistance support technology for the AFR without pillars is then developed. The key components of this technology include macro- and micro-NPR anchor cables.

Macro-PR high-prestress constant-resistance anchor cable

A series of macro-NPR anchor cable support products with a new type of NPR constant-resistance structure was developed in 2008. To compare the mechanical properties of the macro-NPR anchor cable with those of traditional anchor cables, numerous static tensile tests and dynamic impact tensile tests have been carried out. The test results show that the macro-NPR anchor cable has significant constantresistance characteristics, and the maximum displacement of the NPR constant-resistance structure can be up to 1000-2000 mm. The macro-NPR anchor cable is more effective than the traditional anchor cable in terms of the supporting force and maximum displacement, as shown in **Figure 14**.

Micro-NPR high-prestress constant-resistance anchor cable

The micro-NPR support material was developed in 2014 which

Table 1: Comparison of two kinds of roof splitting equipment (He and Zhang, 2018).

Performance index	Bidirectional energy cavity tension blasting equipment	Instantaneous splitting equipment
Explosiveness	Yes	No
Working method	Blasting by detonator	Seal ignition
Required time	Millisecond	0.05-0.5 s
Amount of raw material required for same rock mass	1.15 kg	1 kg
Working mechanism	Detonation wave, shock wave	Expansion of high temperature gas
Heat of combustion	2600e3500 kJ/kg	14,248 kJ/kg
Specific volume	>700 mL/g	306.2 mL/g
Explosion speed	2000e-4000 m/s	Non-explosion
Ignition point	>1 g/cm^3	0.49 g/cm^3
Moisture	<0.5%	0.4%
Flame density	2-8 cm	16.7 cm

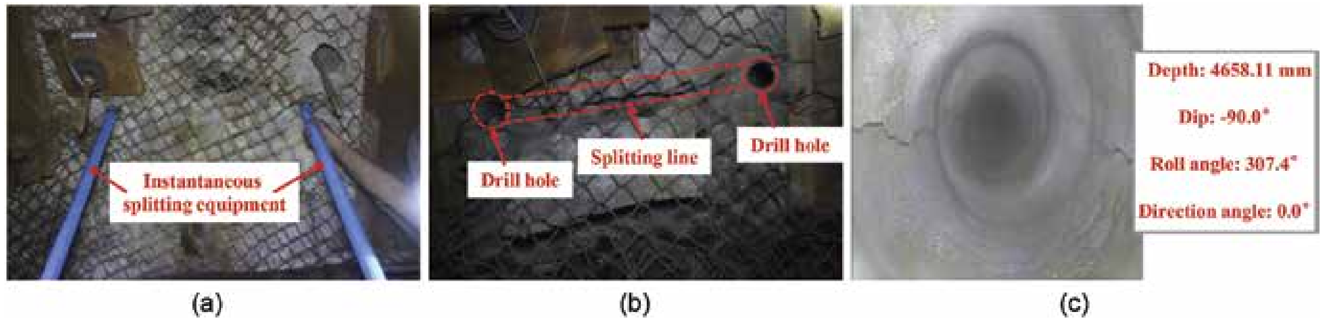

Figure 12: Field test process and effects of instantaneous splitting: (a) Installation; (b) Splitting effect of the hole surface; and (c) Splitting effect of the hole interior.

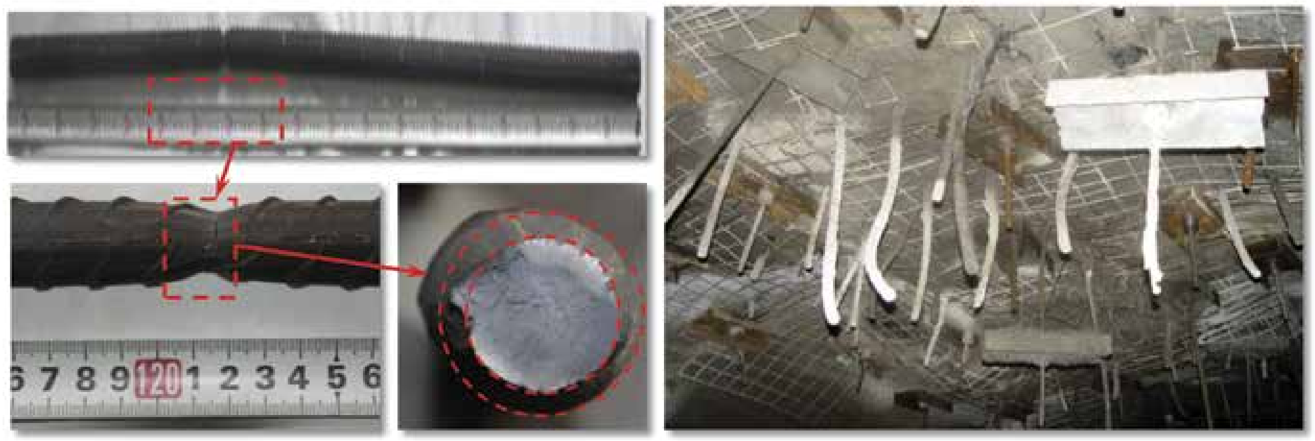

Figure 13: PR effect and failure of traditional anchor cables.

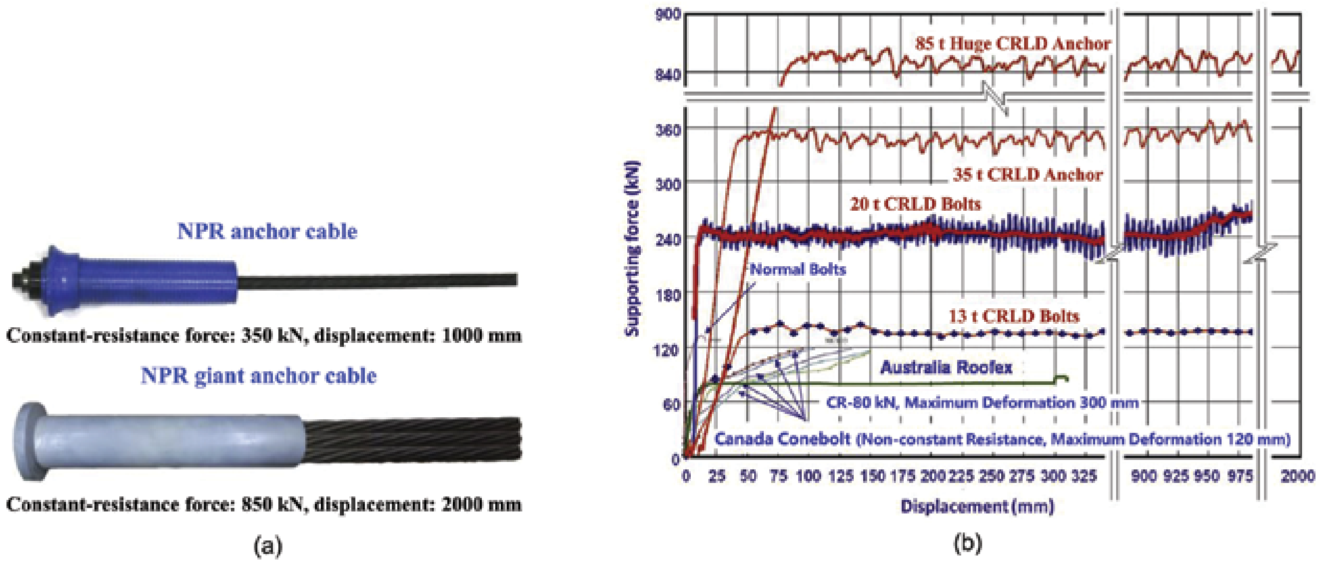

Figure 14: Macro-NPR anchor cable (a) and tensile deformation curve (b) (He, 2006). CRLD represents the constant-resistance large deformation.

is a quasi-ideal plastic material with following advantages:

1. The material has NPR effect, i.e., the PR can reach the magnitude of 10^{-3}.
2. The yield plateau of the material disappears; and
3. The maximum strain of the material is larger than 20%.

The laboratory test results show that the hysteretic energy capacity of the micro-NPR support material is 7-8 times that of the PR support material (Q235 thread steel). The elongation of the added support material can be up to 35%-70%, and the tensile strength ranges from 900 MPa to 1100 MPa. The added support material has better elongation and strength characteristics, and the fracture surface basically has no necking phenomena, as shown in **Figure 15**. The material also has unique properties of non-magnetic, anti-strong magnetic field magnetization and strong anti-corrosion effect.

The micro-NPR high-prestress constant-resistance anchor cable is developed using this new material. This study first realised the NPR effect of anchor cable support products in terms of the material. The design concept of the micro-NPR high prestress constantresistance anchor cable in engineering application is described as follows:

1. The roof anchor cable length. The length of the highprestress constant-resistance anchor cable can be calculated by

Equation 7 $L_H = H_C + 2$

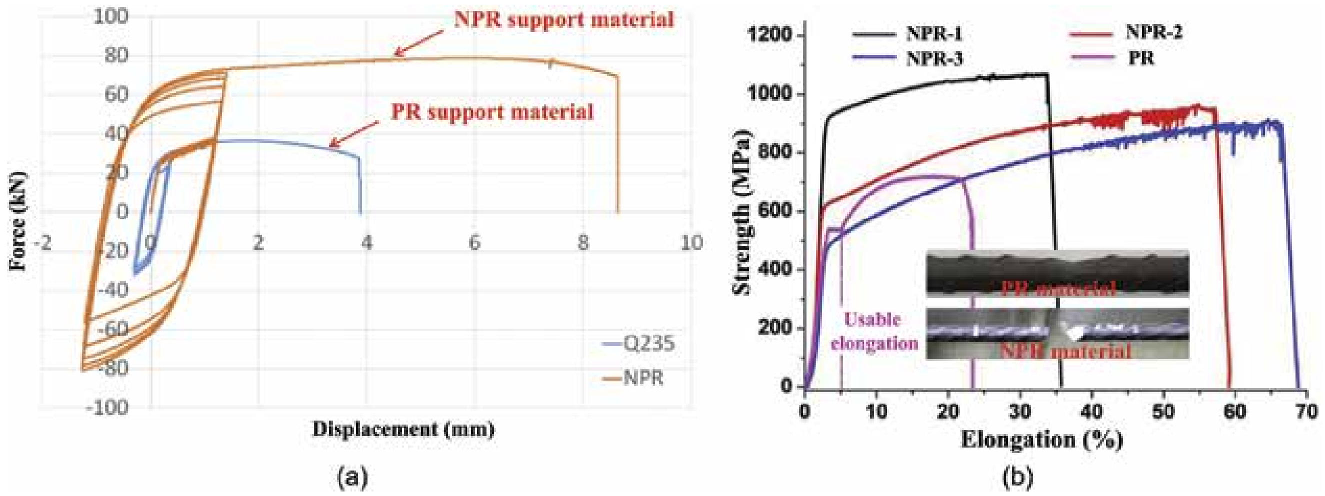

Figure 15: Properties of the micro-NPR support material: (a) Hysteretic energy curve; and (b) Mechanical property curve (He and Xia, 2016).

where L_H is the anchor cable length (m), and HC is the presplitting height (m).

2. The high prestress. The applied prestress of the highprestress constant-resistance anchor cable should be 80%-90% of its ultimate constant-resistance value.
3. The anchor cable number per unit area. The number per unit area of the high-prestress constant-resistance anchor cable, N, can be calculated by

Equation 8 $N = K_c (P_n/P_o)$

where P_n is the roof pressure per unit area (kN); P_0 is the constant-resistance stress of anchor cable (kN); and K_c is the safety coefficient, with the value of 1.1-1.3.

Gangue blocking support technology

High vertical pressure appears on the AFR before the gob roof collapses, and high dynamic pressure will be generated during the collapsing process of the gob roof. For this, the traditional gangue blocking support is prone to bending and slipping, as shown in **Figure 16**. Therefore, a new support technology should be developed, which can resist large forces and control surrounding rock deformation to ensure the stability of the gangue rib. The gangue blocking support technology for the gangue rib is proposed herein in view of the above problems. The roof and rib support equipment, gangue blocking mesh and retractable Usteel are used for the combined support technology, as shown in **Figure 17**.

The roof and rib support equipment are composed of two parts. The first part includes the top beam, bottom beam, push plate and column, which can provide large supporting force to resist roof deformation and maintain yield pressure to adapt to the given deformation of the main roof with the movement process of the overlying strata. The second part includes the upper and lower push plates, providing a large lateral thrust to resist the lateral dynamic load of gangue blocking support during the collapsing process of the gob roof. The retractable U-steel produces a relative displacement under the extrusion action generated by roof subsidence, actively yielding pressure with high resistance to prevent bending instability in the gangue blocking support structure. The collapsed rock mass is piled up to form the wall under the cooperation of the roof and rib support equipment, retractable U-steel and gangue blocking mesh. The gangue rib is formed after the gangue is compacted and stable.

MINING METHOD OF THE AFR WITHOUT PILLARS

The 110 and N00 mining methods are established based

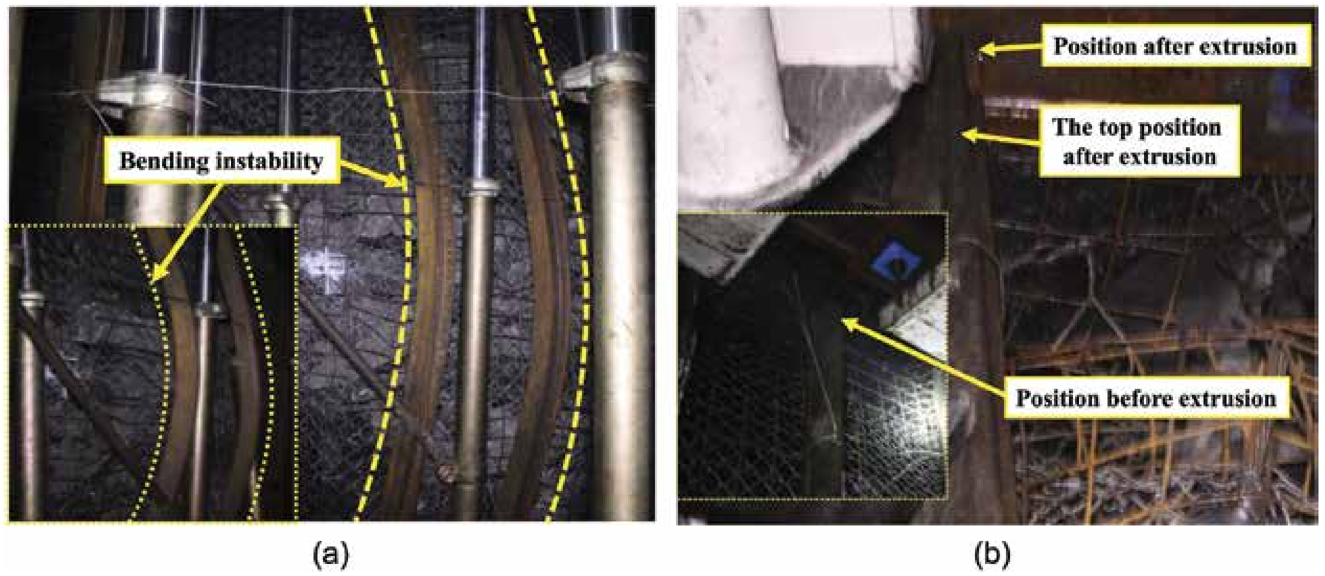

Figure 16: Instability types of common gangue blocking support: (a) Bending instability, and (b) Slipping instability.

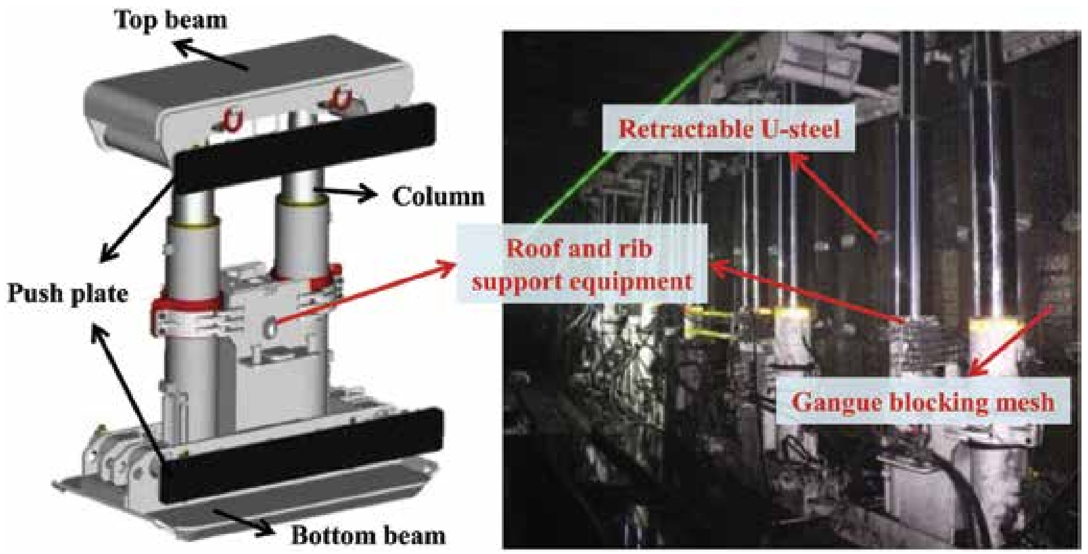

Figure 17: Gangue blocking support equipment of the gangue rib.

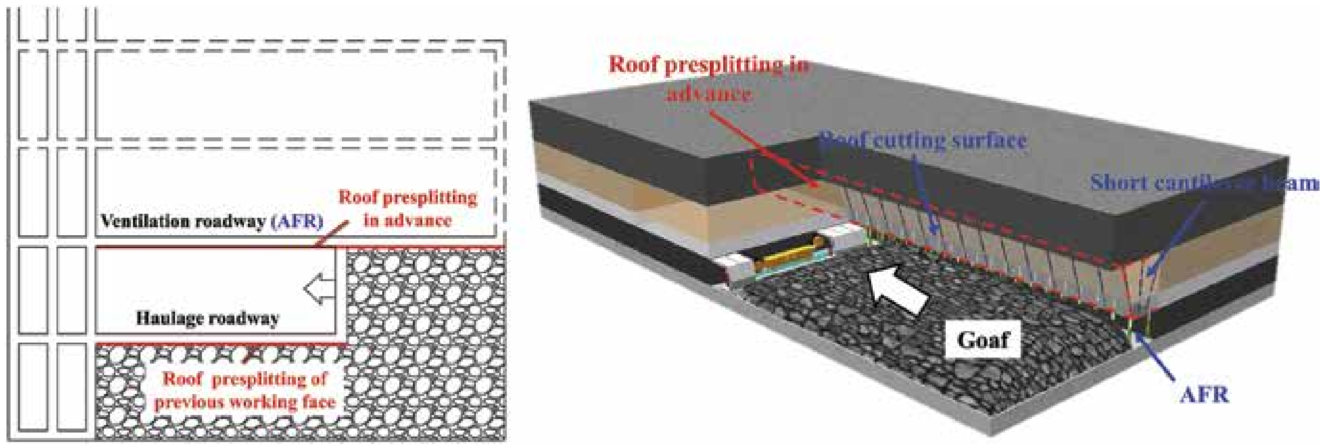

Figure 18: Schematic diagram of the 110-mining method of the AFR without pillars (He, 2009).

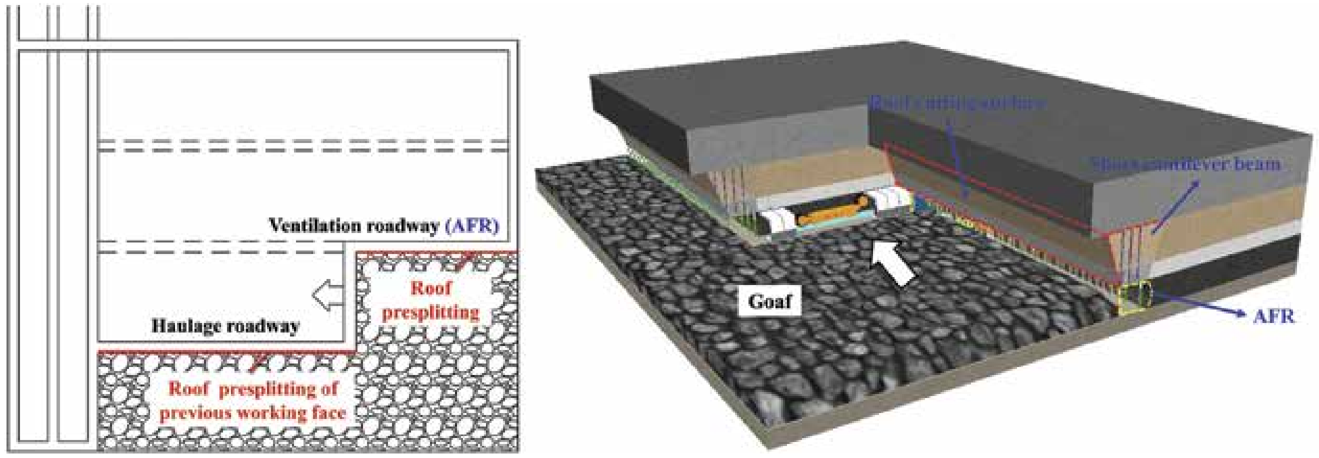

Figure 19: Schematic diagram of the 1G N00 mining method of the AFR without pillars (He and Wang, 2016).

on the "equilibrium mining" theory and the comprehensive application of the key technology of the AFR without pillars.

110 mining method of the AFR without pillars.

The roof presplitting, roof anchor cable support and gangue blocking support are carried out for the reserved roadway in the 10-mining method. The reserved roadway is retained for the next working face, as shown in **Figure 18**. The method can reduce half of the excavation amount of roadway and the coal pillar is not needed, which is beneficial for reducing the stress concentration in the surrounding rocks of roadway. This is an important transition from "in equilibrium mining" to "equilibrium mining."

N00 mining method of the AFR without pillars

1G N00 mining method of the AFR without pillars

The 1G N00 mining method of the AFR without pillars is proposed based on the 110-mining method. In this method, the roadway excavation for the working face is not needed and the integrated mode of coal mining and roadway retaining can be realised, as shown in **Figure 19**. The mining technique, equipment system, and layout of the working face and roadway are changed. The roadway is automatically formed and retained by roof cutting on one side of the working face, and the roadway excavation (except the boundary roadway) and coal pillar reserved in the panel are not required.

2G N00 mining method of the AFR without pillars

The concept of the 2G N00 mining method of the AFR without pillars is proposed based on the 1G N00 mining method to eliminate all roadway excavations in the whole panel, as shown in **Figure 20**. The working face transportation and conveyor systems are turned and overlapped with the 2G N00 mining method. The support time of roof and rib support equipment is advanced, and the integrated design of the drilling and the support is conducted. The roadway is automatically formed and retained by roof cutting on two sides of the working face, and all mining roadway excavations in the whole panel are eliminated. The application of this method is being conducted in the Xintai coal mine in China.

3G N00 mining method of the AFR without pillars

The concept of the 3G N00 mining method of the AFR without pillars is proposed based on the 2G N00 mining method to eliminate roadway excavation in the whole coal mine and realise a new concept of mine construction, as shown in **Figure 21**. The transportation and ventilation systems are formed through the mining of the working face in the 3G N00 mining method. The mine construction is simplified due to the reduction in the mine construction duration, the simplification of the shaft station, and the elimination of the main roadway excavation. The mode of no coal pillar reserve and roadway excavation is realised in the whole mine. All the coal resources can theoretically be mined out, providing that the intelligent and unmanned mining is realised in the whole mine. The application of this method is being conducted in the Xiaohaotu coal mine in China.

4G N00 mining method of the AFR without pillars

The concept of the 4G N00 mining method of the AFR without pillars is proposed based on the 3G N00 mining method to realise intelligent unmanned mining and eliminate mine ventilation, as shown in **Figure 22**. Memory mining with shearers, automatic machinery-tracked systems of hydraulic support and visual remote monitoring are the basis of the 4G N00 mining method. The intelligent control platform is adopted to realise the intelligent control of the whole mine to ensure the continuous, safe, and efficient mining of the working face. Mine ventilation will be eliminated, and gas disasters will be transformed into natural gas resources. The intelligent and unmanned simultaneous extraction of coal resources and natural gas resources will be realised.

Development of the mining method

The 110 and N00 mining methods of the AFR without pillars are coal mining innovations in China, in addition to gob-side entry driving (121 mining method) and gob-side entry retaining (111 mining method). The 121-mining method adopts the "masonry beam theory" and "transfer rock beam theory" (Song, 1979). The mining method of the AFR without pillars follows the "short cantilever beam theory." The 110-mining method and 1G N00 mining method have been successfully applied in the field. The 2G and 3G N00 methods are being conducted in two coal mines in China. The technical characteristics of the 121-mining method, 110 mining method and each stage of the N00 mining method are compared and summarised in **Figure 23**.

ROCK MECHANICS (PART 1)

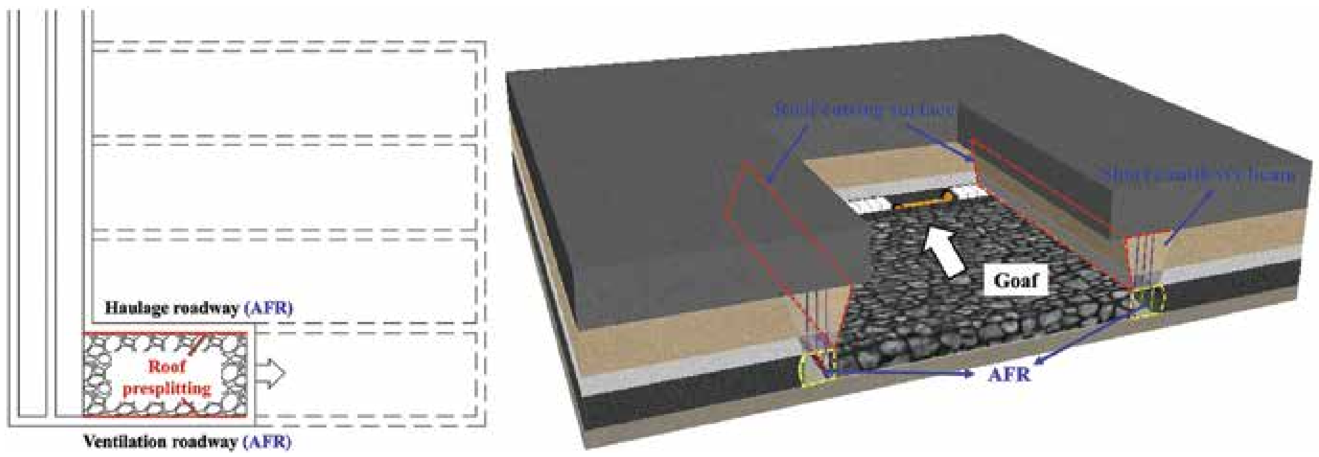

Figure 20: Schematic diagram of the 2G N00 mining method of the AFR without pillars (He and Wang, 2018).

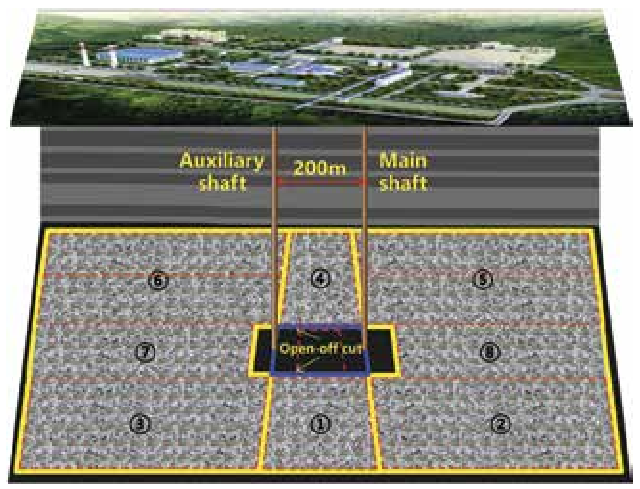

Figure 21: Schematic diagram of the 3G N00 mining method of the AFR without pillars (He and Wang, 2019).

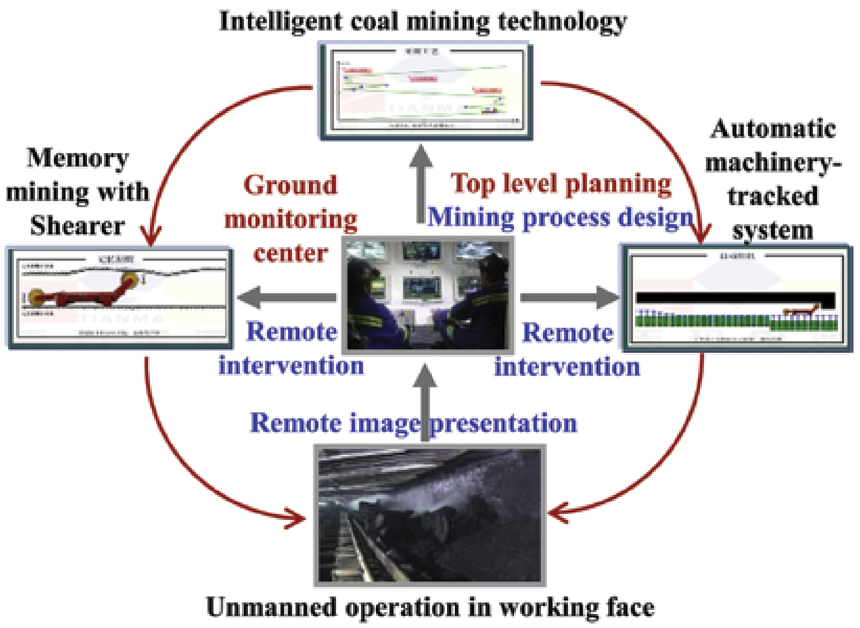

Figure 22: Schematic diagram of the 4G N00 mining method of the AFR without pillars (He and Wang, 2020).

DECLARATION OF COMPETING INTEREST

The authors declare that they have no known competing financial interests or personal relationships that could have appeared to influence the work reported in this paper.

ACKNOWLEDGMENTS

This work was supported by the Natural Science Foundation of China (Grant Nos. 52074164 and 42077267) and the Major Scientific and Technological Innovation Project of Shandong Province, China (Grant No. 2019SDZY04). The authors contributed equally to this paper. Thanks to Prof. Jun Yang, Dr. Yajun Wang, Dr. Bei Jiang, Dr. Yubing Gao, Dr. Hongke Gao, Dr. Zhenhua Jiang, Dr. Yue Wang, Dr. Shuo Xu and Dr. Haojie Xue for their contributions of this paper.

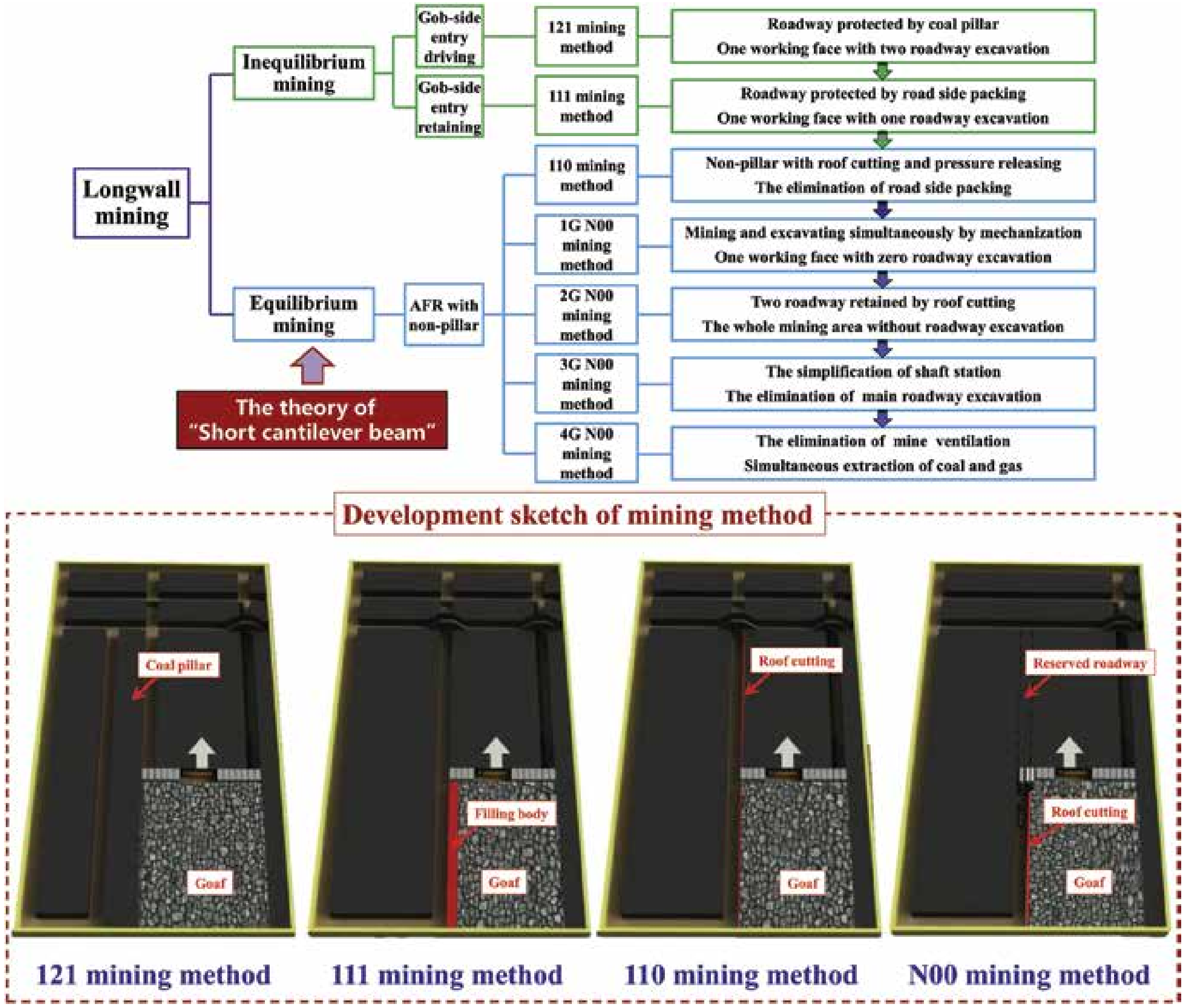

Figure 23: Development and planning of the longwall mining method.

Dr. Manchao is an expert in Mine Engineering and Rock Mechanics. He is an Academician in Chinese Academy of Sciences, professor at China University of Mining and Technology at Beijing (CUMTB), and the vice president at International Society for Rock Mechanics and Rock Engineering (ISRM) of the term 2015e2019. He is the director of the State Key Laboratory for Geomechanics and Deep Underground Engineering, the chairperson of China National Group of ISRM, the president of Chinese Society for Rock Mechanics and Engineering (CSRME), and the chairperson of the Soft Rock Engineering and Deep Disaster Control Subsociety of CSRME. He is also Chief Scientist of the Major Program of the National Natural Science Foundation of China, Chief Scientist of 973 Program and winner of National Outstanding Youth Scholar Fund. He has published four books and over 190 research papers. He also serves on the editorial board member of several journals, including Journal of Rock Mechanics and Geotechnical Engineering

Dr. Qi Wang is professor at China University of Mining and Technology at Beijing (CUMT) and Shandong University. His research focuses on coal mining methods without pillars and the surrounding rock support theory. He is the executive dean of Research Institute for Deep Underground Science and Engineering of Beijing, the director of the Shandong Province Engineering Laboratory of Safety Control for Underground Space. He is also the vice-president at International Society for Rock Mechanics and Rock Engineering (ISRM) Soft Rock Commission, the vice-chairman of Soft Rock Engineering and Deep Disaster Control Subsociety of Chinese Society for Rock Mechanics and Engineering (CSRME). He won the Youth Yangtze River Scholar and the outstanding mid-aged experts in Shandong Province. He took charge of 4 National Natural Science Foundation of China (NSFC) and twenty-one projects from enterprises and institutions. Up to now, he has published 75 SCI- or EI-indexed papers as the first or corresponding author and hold 36 Chinese invention patents as the first inventor.

Quality matters – an essential reference guide to conveyor belt selection

Not all conveyor belts are created equal. In this special feature for Mining & Quarry World, specialist Leslie David examines the criteria used to assess the properties and characteristics of single and multi-ply rubber conveyor belts and the influence each part of the criteria has on whether or not a belt will be fit for its intended purpose.

A COMPLICATED SUBJECT

Industrial conveyor belts appear to be very simple structures to the casual observer. In very basic terms, they are simply thick bands of black rubber that run around metal conveyor frames. They transport a multitude of different ores, minerals and other loose materials thereby performing a hugely important role. In reality however, conveyor belts are technically very complex. Literally billions are spent around the world every year buying, fitting and running them but much can go wrong (and often does!) when a belt is not up to the task it was chosen to perform.

THE TECHNICAL DATASHEET

Selecting a conveyor belt involves making a complicated assessment of all available parameters including the conveyor system itself, the materials being conveyed, the working conditions and health & safety. For new conveyor installations the first stage of any belt selection should involve the use of a belt calculation program overseen by a professional conveyor belt engineer. It can also be a good idea to follow the same process when a conveyor is proving to be problematic. It is important to be absolutely sure that the actual specification of the belt is correct in the first place.

Good belt selection involves making an assessment based on quite a wide-ranging criteria. To be honest, for many people who work with conveyors, much of the criteria is meaningless to them although they would understandably be reluctant to admit it. All responsible manufacturers, service companies and traders should, as a matter of course, provide a technical datasheet (TDS) for the specific version of the belt that they are proposing to supply because this is where much of the selection criteria should be found. The TDS should be supported by the manufacturer's product documentation (product specific datasheet) because this should contain important additional information such as recommended minimum and maximum pulley diameters and maximum useable widths.

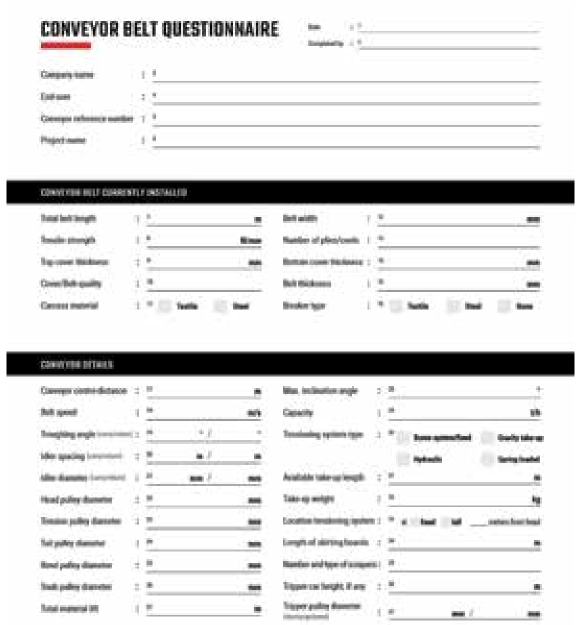
CONVEYOR BELT QUESTIONNAIRE

The first stage of any belt selection should involve the use of a belt calculation program overseen by a professional conveyor belt engineer.

My best advice is to always insist on seeing a technical datasheet and a product datasheet before you place an order for a belt. Even the design and clarity of the documents can be a good indicator as to the professionalism of the supplier you are dealing with. It is also wise to request a certificate of (manufacturers) origin so that you know the true provenance of the belt in the event of a problem.

TEST METHODS AND TEST STANDARDS ARE NOT THE SAME

Alongside each part of the criteria on the technical datasheet should be details of any applicable test methods and international standards such as ISO or DIN for example. When assessing quality credentials it is essential to differentiate between what is simply an approved method of conducting a particular test (the test method standard itself) and the actual quality or performance standards attained during that test. In itself, the fact that a belt has been tested according to a certain method actually means very little. What is important is the actual level of performance achieved during the testing compared against the minimum acceptable level of performance dictated by the test standard. In other words, was the performance standard achieved?

Unfortunately, unless specifically stated otherwise, technical datasheets provided by manufacturers and traders almost invariably only show generic information such as the *minimum* standard demanded by a specific test. Some do show a few 'actuals' but it is extremely limited. The data therefore does NOT reflect the actual performance achieved during the test or even a level of performance that the buyer might reasonably expect. This even applies to the dimensional measurements and acceptable tolerances such as the actual thickness of the top and bottom covers. Apart from Dunlop in The Netherlands, who show actuals on their technical datasheets on most applicable values, this shortcoming applies to all suppliers.

The vast majority of conveyor belts in use today are either single ply or, most typically, multi-ply. For the benefit of the uninitiated, their construction consists of two elements – a fabric ply carcass, most commonly Polyester warp and Polyamide (nylon) weft (EP) fabrics, with a thin layer of rubber in between the plies (skim rubber or inter-ply rubber). This structure is covered by an outer layer of rubber on both sides referred to as 'the covers'. Technical datasheets are therefore based on these two fundamental elements. Each element has its own criteria for testing methods and performance standards. On most technical datasheets, data relating to the carcass is usually shown first.

THE CARCASS

The carcass provides the innate strength of any conveyor belt. It not only has to bear the loads placed upon it but also repeatedly flex around the drums and pulleys of the conveyor structure. The internal structure of the belt carcass dictates the tensile strength of the belt. Because of its fundamental importance, the tensile strength is usually the first piece of data shown on a technical datasheet.

Selection criteria – Tensile strength at break (N/mm)

Virtually all industrial conveyor belts are defined by their tensile strength. The carcass absorbs the force when tension is applied to the belt. The greater the required tensile force to move the transported material, the greater level of strength demanded of the belt carcass. Importantly, the strength under load needs to be consistent throughout the belt both longitudinally and transversely in order for the belt to steer and handle correctly. The tensile strength of a belt is measured according to the ISO 283 test method. Quite simply, this involves pulling a section of belt apart and measuring the force that it will endure before it breaks.


The tensile strength of a belt is measured according to the ISO 283 test method.

As I touched on earlier, a typical technical datasheet will simply state the minimum tensile strength that the manufacturer/supplier is claiming the belt will achieve. A poor quality belt will often be borderline and, due to inconsistencies in the production process and the quality of the fabric plies used, sometimes below the required minimum strength. When competing on price, manufacturers will habitually keep every aspect of the construction cost to an absolute minimum. The better quality conveyor belts will have a safety margin included, ideally as much as 10% or more.

Selection criteria – Carcass Tear Strength (N)

Depending on the working environment and the kind of materials being conveyed, the overall tear strength of a conveyor belt can be hugely important. For clarity of meaning, a 'tear' is best defined as what happens when a piece of material (a section of carcass or rubber cover) is pulled apart in opposing directions. Although there is a defined method of testing (ISO 505: 2017) there are no standardised performance requirements.

The test consists of mounting two cut ends of a test piece of belting or rubber cover in the jaws of a tensile testing machine. An initial tear is made in the test piece, which is then pulled apart in opposing directions. The force necessary to propagate the tear is then measured. Examination and analysis of the multi-peak tear resistance test traces is conducted in accordance with ISO 6133.

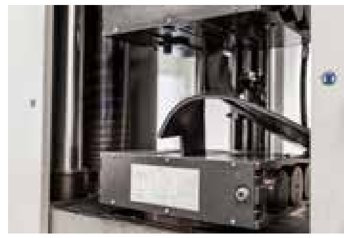
ISO 505 tear strength testing.

Selection criteria – Adhesion between the plies

The strength of adhesion (bond) between the various layers of plies and between the plies and the covers is also a standard part of the assessment criteria. The adhesion (measured according to the ISO 252 test method) literally involves pulling the layers apart and measuring the force required in Newtons per millimeter.

When it comes to adhesion, manufacturers need to strike a balance because there should obviously between a strong bond between all of the layers so that the belt stays intact under load and while being subjected to repeated flexing.

Measuring adhesion literally involves pulling the layers apart and measuring the force required.

The belt carcass plays a vital role in minimising the effects of impact and trapped sharp objects.

The use of EE fabrics instead of EP reduces troughability, impact resistance and rip resistance.

However, if the adhesion level is too high then this can create problems when trying to make a spliced connection joint because a section of the rubber skim needs to be removed.

Selection criteria – Thickness

The measurement method for carcass thickness is ISO 583. The actual thickness of the carcass largely determines the suitable usage range for the belt. A very thin carcass will require less material to manufacture and be cheaper in cost. It will typically be easy to flex around pulleys and be able to take a troughed shape in narrow width conveyor frames. However, being thin and flexible also makes the belt more sensitive to damage from material impact and sharp edges. The thickness of a carcass can be increased simply by increasing the amount of rubber between the fabric plies. The downside to this is that it will become more rigid and could prove to be problematic and actually lead to internal damage within the carcass.

With larger width belts and bulky, heavy material dropping on the belt from height, the extra rigidity created by increasing the thickness will provide added resistance to these elements. In reality, quality manufacturers try to match the most commonly expected usage of a belt type to the carcass design for each specific belt type and strength. In other words, making the carcass thick and rugged enough but without limiting the application area by being too thick or too thin.

Selection criteria – Elongation

The elastic elongation (stretch properties) of a carcass are more important than many people may realise. Using test method ISO 283, the amount of elongation is measured while the test piece is under a tension that is the equivalent of 10% of the stated tensile strength. Again, a balance has to be achieved because the belt needs to be able to accommodate geometric changes such as pulleys and transitions. On multi-ply belts, insufficient elongation can lead to shear stresses, which in turn can cause delamination issues. However, too much elongation would result in insufficient tension in the belt.

Generally speaking, the maximum elongation (at maximum operational tension, being 10% of the nominal belt breaking strength) for multi-ply belts would be 1.5% for lower tensile belts, max. 2.5% for the mid-range and 3% for the really high tension belts. Personally, I would not expect to see much more than 1% in the lower range and 2% in the high tension classes. Anything appreciably less than that would mean that the belt is more sensitive to dynamic failure and more prone to damage.

Resisting damage

Crucially, the carcass and the fabrics that are used within it play a very important role in handling (dissipating) the impact of objects falling on to the belt and also resisting the propogation of tearing and ripping when objects become trapped and penetrate the outer covers. This is a key reason why Polyester warp and Polyamide weft (EP) fabrics are most commonly used. Although not part of the criteria used within a technical datasheet, the type of fabric used will be stated on the document as part of the belt designation. For example, EP 400/3 4+2.

Worringly, laboratory testing is revealing that more and more belts, including many that are being manufactured in Europe, are being declared as having an EP (polyester/nylon mix fabric) construction when they actually have entirely polyester (EE) fabric plies. A simple one-on-one replacement of the Nylon with Polyester is not possible due to the lower elasticity of Polyester because it would lead to a very rigid carcass with a significant reduction in troughability. A belt that will not seat properly often results in misalignment of the belt relative to the conveyor structure. Therefore, a much lower amount of polyester weft material is used in the exchange. A direct consequence of less material of lower elasticity is that impact resistance and rip resistance are markedly reduced, making the belt even more vulnerable to damage than usual.

The objective of using purely polyester fabric is to minimise costs because polyester costs some 30% less than nylon. Although a highly tempting price may provide a clue, the deception cannot be detected without laboratory testing so the manufacturers are confident that their dishonesty is very unlikely to be exposed.

INDUSTRIAL CONVEYOR BELTS

THE COVERS

In the majority of cases, the quality of the outer covers have the greatest influence on the performance and operational lifetime of a conveyor belt. This most certainly applies in the case of belts that need to be able to resist the ravages of heavy, sharp, abrasive materials, high material temperatures or where the conveyed product contains oil of any kind. Within this, the ability of the rubber covers to resist abrasive wear will have a very significant bearing on the wear life of the belt. The destruction of the covers will allow the carcass materials to be exposed, which will then gradually deteriorate and lose integrity and strength. This will eventually lead to rupture of the belt and costly downtime and spillage.

Selection criteria – Abrasion resistance [mm^3]

The two most commonly referenced standards for fabric reinforced belting are the international ISO 14890 (with abrasion resistant classes H, D and L) and German DIN 22102 (with abrasion resistant classes Y, W and X). In Europe the longer-established DIN 22102 standard is still very often used, although the most current version of this standard references the ISO 14890 on most topics, making both more or less identical. Generally speaking, the DIN grade “Y” (or ISO 14890 closest equivalent grade “L”) relates to ‘normal’ service conditions and DIN grade “W” (close to ISO 14890 grade “D”) for particularly high levels of abrasive wear. DIN grade “X” (close to ISO 14890 grade “H”) is regarded as the most versatile because in addition to resisting abrasive wear it also has good resistance to cutting, impact (from high drop heights) and gouging, usually caused by heavy, sharp materials. To achieve these characteristics the rubber compound contains a higher than usual element of natural rubber (NR) and is therefore usually the highest priced option.

The method used to measure abrasion resistance (ISO 4649 / DIN 53516) involves moving a test piece of the rubber across the surface of an abrasive sheet mounted on a revolving drum and is expressed as volume loss in cubic millimeters, for instance 150 mm^3.

The key factor to bear in mind when looking at abrasion test results is that higher figures represent a greater loss of surface rubber, which means that the higher the figure the lower the resistance to abrasion. Conversely, the lower the figure the better the wear resistance.

Selection criteria – Tensile strength at break (MPa)

The tensile strength of belt covers is measured according to the ISO 37 test method and is typically expressed as amount of force in megapascals (typical range of 15-30 MPa). During this test, the material is stretched up to the point of failure. This point of rupture (referred to as the ultimate tensile strength) indicates how much force or stress the rubber can withstand before breaking and has considerable influence on the overall tensile strength of the belt. As I mentioned earlier, technical datasheets provided by manufacturers almost invariably only show the minimum standard demanded by a specific test or, in many cases, simply the test method reference number and nothing more. This therefore does not reflect the level of performance that you might reasonably expect.

Selection criteria – Elongation at break (%)

The elongation at break is the extent a rubber material can be strained (%) before it breaks. Using ISO test method 37, tensile force is exerted in order to stretch the rubber to breaking point. The elongation at break is expressed as a percentage percentage of the original length of the test piece.

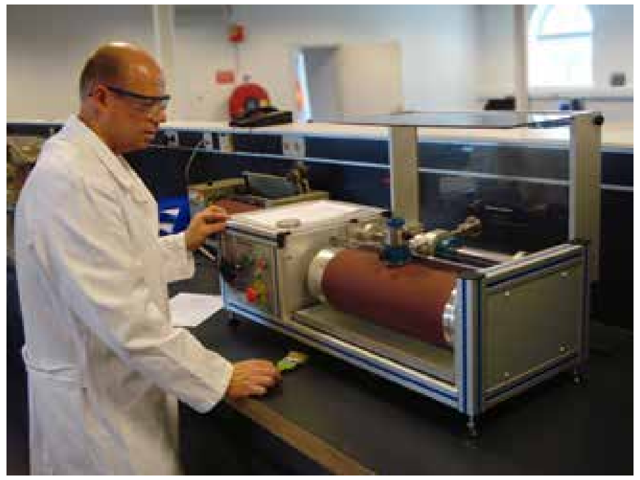

ISO 4649 / DIN 53516 abrasion testing.

The elongation of the covers has an important bearing on the elongation properties of a belt as a whole.

As with the tensile strength, the elongation of the covers also has an important bearing on the elastic elongation properties of the belt as a whole. This means that even if the carcass has good mechanical properties, if the quality of the rubber covers is poor then this will have a seriously detrimental effect on overall performance, handling and the ability of the belt to withstand physical punishment (such as heavy, sharp material falling from height) and rip and tear propogation. Typically, some 70% of a conveyor belt is made up of rubber so despite its critical role, it is usually the primary target for cutting corners.

Selection criteria – Tear strength [N] / [MPa]

Testing the tear strength of the rubber covers is similar to the testing of tensile strength. The difference is that a specifically designed and pre-damaged sample is pulled until it breaks. The damage acts as an initiation to a further tear and inevitable break of the sample. The sample will typically break at a lower tension than the undamaged sample.

In real life, the covers of a conveyor belt will be damaged by material impact. When the tear strength is low, these small areas of damage become larger areas of damage as a result of the strain placed on the covers by continuous flexing around pulleys and drums. However, rubber

Ozone & ultra violet light causes rubber to literally disintegrate

covers with a high level of tear strength will contain the damage much more effectively, thereby achieving a longer operational life. Although international standards only focus on the ultimate tensile strength, evaluating the tear strength in combination with the expected operational conditions of the belt is a worthwhile exercise. Belts conveying large and sharp materials greatly benefit from a cover rubber that has both good tensile strength and high tear strength.

Selection criteria – Hardness (Shore)

The hardness of rubber covers is usually measured by the depth of indentation caused by a rigid ball under a spring load or dead load (ISO 7619). The spring-loaded meter gives Shore A values of hardness ranging from 0 to 100. For the majority of rubber cover grades a hardness of between 60 to 65 Shore is the expected norm.

As with the degree of elasticity (elongation), there is a relatively fine balance that needs to be achieved by the manufacturer because anything outside of this range can make the covers prone to damage. Although soft rubber covers may provide better damping on impact, the greater amount of deformation will still make it subject to damage. Conversely, a hard cover may eventually lack the ability to allow bigger deformations because over the course of time, all rubber materials become harder and lose flexibility as a result of ageing. This natural ageing process is accelerated when belts are subjected to heat or chemicals.

Selection criteria – Ozone & ultra violet light resistance (EN ISO 1431/1 procedure B)

Despite its crucial importance in terms of operational lifetime, resistance to the damaging effects of ozone and UV is rarely ever mentioned by traders or manufacturers in their product documentation. This is almost certainly because the anti-ozonants that need to be used during the mixing process of the rubber compounds are relatively costly. Ozone becomes a pollutant at ground level and exposure is unavoidable. It increases the acidity of carbon black surfaces and causes reactions to take place within the molecular structure of the rubber resulting in surface cracking and a marked decrease in its tensile strength.

Likewise, ultraviolet light from sunlight and artificial (fluorescent) lighting also accelerates deterioration because it produces photochemical reactions that promote the oxidation of the surface of the rubber resulting in a loss in mechanical strength. In both cases, this kind of degradation causes the covers of the belt to wear out even faster than they should so my advice is to always make ozone & UV resistance a required part of the specification when selecting any rubber conveyor belt.

Blind acceptance of promised quality can prove to be extremely expensive

Blind acceptance

Because of the everyday pressures of working life and, indeed, budgetary pressures, it is very easy to fall into the trap of simply accepting that the specification being promised by the belt supplier will be what you actually receive on site. The same applies to the level of performance and quality standards claimed by the supplier. As I explained earlier, just because there is a test method or quality standard reference shown alongside a particular characteristic it does not necessarily mean that the belt supplied will actually meet that standard.

This may sound very cynical but blind acceptance can prove to be extremely expensive. Naturally, there should be an element of trust in any transaction. However, it is important to consider the growing evidence of misleading information right through to outright deception in the conveyor belt industry.

Taking the time to study the technical datasheet (TDS) for the specific belt you are being offered, together with the manufacturer's product specification datasheet before you place the order will certainly be time well spent.

ACKNOWLEDGMENTS

Conveyor belt selection is a massive topic involving a complicated assessment of all available parameters relating to the actual conveyor system, materials being conveyed and numerous belt specification options. Although I have tried to 'keep to the basics', it has nonetheless been a challenging task. I am therefore deeply indebted to Rob van Oijen, manager of application engineering for Dunlop Conveyor Belting in The Netherlands for his invaluable technical and professionally impartial assistance in the compilation of this article.

ABOUT THE AUTHOR

Leslie David

After spending 23 years in logistics management, Leslie David has specialised in conveyor belting for over 15 years. During that time, he has become one of the most published authors on conveyor belt technology in the world.

EnergyAustralia pledges to ditch coal by 2040, closing coal-fired power stations

One of the biggest power plants in New South Wales will shut earlier than planned as EnergyAustralia pledges to move away from coal by 2040.

Key points:

- A coal-fired Lithgow power station likely to be the last operating NSW will shut at least two years earlier than planned
- EnergyAustralia's announcement comes a day after China declared it would no longer invest in overseas coal assets
- The closure is likely to have a significant impact on Lithgow, which is a traditional mining town

The company will close the Mount Piper Power Station, near Lithgow, by 2040.

The station, which was due to shut in 2042, provides energy to almost 1.2 million homes in NSW and is fuelled by black coal sourced from local mines.

Mount Piper is the state's newest power station.

EnergyAustralia managing director Mark Collette said the move to renewables would have "significant impacts for our power station workers and our local communities".

Coal mining is historically one of the most important industries to the Lithgow economy and employs about 75% of the town's population.

"While Mt Piper's ultimate retirement date will be determined by several factors, we are committed to long-term planning and supporting the transition for our workers and our local communities," Mr Collette said.

China consumed twice as much energy as the European Union in 2018

Green wave

The announcement comes a day after the Chinese government pledged to stop funding coal projects abroad.

The world's largest greenhouse gas emitter has vowed to become carbon neutral by 2060.

Green Energy Markets and Institute for Energy Economics and Financial Analysis predicted Mount Piper will be the last coal-fired power station running in the state.

The organisations expected the station would be running at a loss as early as 2025.

This week, according to the OpenNEM, Australia's reliance on wind, solar and hydro power reached an all-time high of 60.1%.

Historic change

The region's biggest coal supplier, Centennial Coal, which owns and operates two mines that supply the power station, told the ABC the pledge will have no impact on its existing operations.

Springvale Coal Mine, which directly supplies the local station and has a workforce of nearly 400 people, is set to shut in 2024.

It has withdrawn plans to reopen and expand the Angus Place colliery near Lithgow, which came up against major opposition over its impact on the surrounding environment, including endangered swamps.

It comes after Centennial Coal's Thai-based parent company Banpu announced in July it would no longer invest in new coal assets, but did not rule out modifying existing licences.

The company has now submitted a new proposal to the state's planning department for the expansion of an underground mine.

That mine, known as Angus Place West (separate from the Angus Place colliery) would supply the Mount Piper Power Station for the remainder of its lifetime – a window that appears to be rapidly closing.

Earthquake halts operations at Victorian gold mine

White Rock Minerals has suspended underground operations at its Woods Point gold project after an earthquake struck near Mansfield in Victoria.

Located 60km south of the estimated epicentre, the Woods Point operation reported significant shaking on site at the time of the earthquake.

Nine workers were underground at the time and all personnel are safe, accounted for and are now all back on the surface.

White Rock reported no immediate damage on site at Woods Point and the company is currently following emergency response protocols.

The company has also devised an inspection plan for site and underground infrastructure.

White Rock stated there is no plan to immediately return to underground activities until the aftershocks have subsided.

The company will also wait until the site integrity has been consolidated and inspections have confirmed no damage.

The earthquake struck at 9:15am AEST in the morning, occurring 10km beneath the surface at a magnitude of 5.9, according to Geoscience Australia.

It is understood the tremor was felt across Victoria, in Canberra and in parts of New South Wales.

A spokesperson for the Minerals Council of Australia said no damage or injuries had been reported at Victorian mines in the wake of the earthquake.

Other mines in the area include Morning Star mine, located within the Walhalla to Woods Point goldfield, and the A1 mine about 23km south-east of Jamieson.

Morning Star is operated by AuStar, which was acquired by White Rock in February this year, while A1 is operated by junior gold producer Centennial Mining, which was acquired by Kaiser Reef in January this year.

Hudbay finds three new deposits at Copper World

Toronto- and New York-listed Hudbay Minerals has identified three new deposits at its Copper World project, located on wholly-owned private land in Arizona. This now takes the project's deposits to a total of seven, covering a combined 7 km with mineralised occurrences.

"Our 2021 drill programme at Copper World proved that the previously discovered deposits remained open along strike, and we are highly encouraged by the identification of three new deposits in the area," said president and CEO Peter Kukielski.

The programme has consisted of condemnation, exploration and confirmation drilling over the company's patented private land claims at Copper World. As of June 30, about 166 holes were completed totalling more than 91 000 ft of drilling. As of August 31, Hudbay has received and validated the assay results for 130 of these holes and the results continue to exceed the company's expectations.

The programme resulted in the discovery of three new deposits, including significant volumes of high-grade copper sulphide and oxide mineralisation starting, in most cases, near surface or at shallow depth. These three new deposits are called Bolsa, South Limb and North Limb.

The program also confirmed and increased the confidence in the size and quality of the Copper World, Broad Top Butte, Peach and Elgin deposits.

Drill hole 186 intersected 263 feet of 1.11% copper starting from surface, drill hole #190 intersected 205 feet of 1.39% copper starting from surface, drill hole #191 intersected 404 feet of 1.50% copper starting from surface, drill hole #139 intersected 125 feet of 1.34% copper, drill hole #177 intersected 121 feet of 1.32% copper and drill hole #118 intersected 160 feet of 1.15% copper.

"Copper World is growing into an attractive copper development project in our organic pipeline, and we remain on track for an initial inferred resource estimate before the end of the year and a preliminary economic assessment in the first half of 2022," said Kukielski.

Hudbay sees Copper World as a "very interesting, either alternative or add-on" to the adjacent Rosemont project, which continues to be in legal limbo.

Maptek makes geological modelling simple

Making geological modelling simple is the premise of Vulcan GeologyCore, released by technology developer Maptek.

Vulcan GeologyCore answers the need for an intuitive geological modelling workflow that handles automatic validation and chart creation, providing geologists with greater confidence around their domain and modelling decisions.

The dynamic interface and streamlined workflow make it easy to test different domaining scenarios and view live statistics, before proceeding to the preferred modelling method. Customers can choose from implicit or vein modelling in Vulcan or easily access the machine learning engine in DomainMCF.

'As a geologist, I sum up the impact of Vulcan GeologyCore from the belief that our time is better spent making decisions about geology, rather than in specification setup!' said Richard Jackson, Vulcan Geology Team Lead at Maptek.

Vulcan GeologyCore harnesses interactive drillhole visualisation, lithology targeting and modelling algorithms for narrow vein, disseminated or stratigraphic deposits.

A significant benefit of the new Maptek approach is the streamlined data management. The process sets up project data in a reliable, validated way, removing manual data validation and manipulation.

'A key driver for this solution was a desire to offer our customers a reduced technology barrier to start actual modelling,' said Jackson.

Geologists continue to cite data validation as the biggest hurdle in the modelling process, and also the greatest imposition on their time.

Vulcan GeologyCore liberates geologists from step-by-step procedural tasks that increasingly can be automated, freeing them up for higher value analysis.

Improving the geological modelling process has flow-on benefits. Vulcan GeologyCore means resource and production models can be updated more frequently, easily and confidently.

Vulcan GeologyCore was one of the tools provided to participants in the 2021 Maptek Geology Challenge. The winner, Henry Dillon, Senior Geologist from Golder Associates, applied a combination of Vulcan GeologyCore and DomainMCF to model complex lithologies in a braided river system.

As well as displaying an innovative approach to geotechnical assessment of performance and design for the foundation of a future structure, Dillon provided invaluable feedback for improving the integrated Maptek solution for all users.

'Our ultimate goal is to make solutions simple to set up and use so that our customers can realise the value arising from their geological data,' concluded Jackson.

Vulcan GeologyCore is incorporated in Vulcan GeoModeller and GeoStatModeller bundles and available as a standalone subscription for new customers.

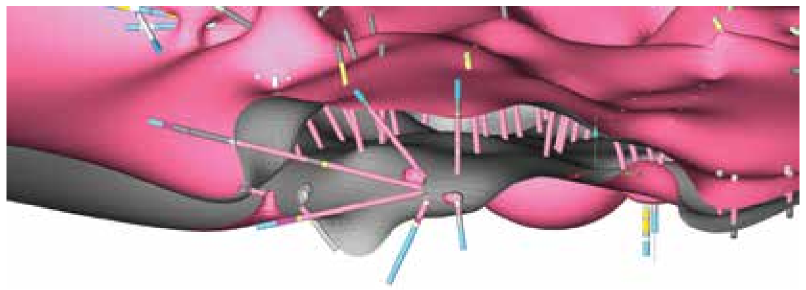


NEW TD-15M
A CUT ABOVE THE REST
WORK SMARTER NOT HARDER
WITH AN ALL-NEW FIRST CLASS CAB
SEE MORE, DO MORE WITH 33% MORE VISIBILITY
ELECTRO-HYDRAULIC JOYSTICKS FOR PRECISE COMMAND & CONTROL
DIGITAL READY FOR CHOICE OF CONNECTED GRADE CONTROL SOLUTIONS
RANGE OF BLADES & RIPPERS DESIGNED TO PUSH THE LIMITS
FIND OUT MORE: Email INFO@DRESSTA.COM or visit WWW.DRESSTA.COM
DRESSTA
ENGINEERED FOR YOUR BUSINESS